Ore Geology Reviews 84 (2017) 185–201

Contents lists available at ScienceDirect

Ore Geology Reviews

journal homepage: www.elsevier.com/locate/oregeo

Structural setting for Canadian Malartic style of gold mineralization in the Pontiac Subprovince, south of the Cadillac Larder Lake Deformation Zone, Québec, Canada

Stéphane Perrouty [a,*], Nicolas Gaillard [b], Nicolas Piette-Lauzière [c], Reza Mir [d], Marc Bardoux [e], Gema R. Olivo [f], Robert L. Linnen [a], Charles L. Bérubé [g], Philip Lypaczewski [h], Carl Guilmette [c], Leonardo Feltrin [a], William A. Morris [i]

[a] Western University, Department of Earth Sciences, 1151 Richmond Street, London, ON N6A 6B7, Canada
[b] McGill University, Department of Earth and Planetary Sciences, 3450 University Street, Montréal, QC H3A 0E8, Canada
[c] Université Laval, Département de Géologie et de Génie Géologique, Québec, QC G1V 0A6, Canada
[d] Laurentian University, Department of Earth Sciences, 935 Ramsey Lake Road, Sudbury, ON P3E 2C6, Canada
[e] Barrick Gold Corporation, 161 Bay Street, Suite 3700, Toronto, ON M5J 2S1, Canada
[f] Queen's University, Department of Geological Sciences and Geological Engineering, Kingston, ON K7L 3N6, Canada
[g] École Polytechnique Montréal, Département des Génies Civil, Géologique et des Mines, 2900 Boulevard Edouard-Montpetit, Montréal, QC H3T 1J4, Canada
[h] University of Alberta, Department of Earth and Atmospheric Sciences, Edmonton, AB T6G 2E3, Canada
[i] McMaster University, School of Geography & Earth Sciences, 1280 Main Street West, Hamilton, ON L8S 4L8, Canada

ARTICLE INFO

Article history:
Received 29 September 2016
Received in revised form 3 January 2017
Accepted 11 January 2017
Available online 12 January 2017

Keywords:
Abitibi
Pontiac
Canadian Malartic
Structural interpretation
Cadillac break
Gold

ABSTRACT

The structural setting of the Pontiac Subprovince in the vicinity of the world-class Canadian Malartic gold deposit has been revisited by combining and reinterpreting airborne geophysical surveys together with a century of structural observations. Felsic-intermediate intrusive bodies are a key component of this deposit. Defining the regional and local favorable structural setting for intrusive rock emplacement within the clastic meta-sedimentary rocks of the Pontiac Group, south of the Cadillac Larder Lake Deformation Zone, may further assist gold exploration in similar tectonic environment.

Three structural domains are interpreted in the area based on the geometry of the bedding, folds and structural fabrics related to the three major phases of deformation. During these events four phases of magmatism and one metamorphic episode occurred. The North domain, which hosts the Canadian Malartic deposit, is characterized by highly variable bedding orientations produced by the interference patterns of isoclinal F_1 folds overprinted by open to tight, steeply dipping, F_2 folds. The bedding in this domain is cut by a penetrative S_2 biotite foliation, which possibly built on rheological changes enhanced by metasomatism in the footprint of the Canadian Malartic deposit. By contrast, the Central and South domains display homogeneous bedding orientations cross-cut by a discrete S_2 biotite foliation and syn- to late- D_2 metamorphic porphyroblasts. In all domains the L_2 stretching lineation consistently plunges at about 60 degrees toward the east. D_3 is a minor deformation event in the Pontiac Subprovince, which possibly correlates with late dextral transcurrent movement along the Cadillac Larder Lake Deformation Zone.

Intrusive bodies were emplaced throughout the first and second deformation events. Phase 1 monzonite, quartz-monzodiorite and granodiorite plutons (ca. 2683–2680 Ma) intruded into consolidated Pontiac sedimentary rocks during D_1. Phase 2 quartz-monzodiorite bodies (ca. 2679–2676 Ma) predominantly formed in the North Domain along F_1 fold axial surfaces prior to or at the onset of D_2. Phase 3 basic dykes (ca. 2675–2673 Ma) cross-cut earlier felsic-intermediate intrusions across all domains and subsequently developed an S_2 metamorphic hornblende foliation. Phase 4 magmatism (ca. 2672–2662 Ma) is related to the Décelles Batholith S-type granite and pegmatite, which is interpreted to be contemporaneous with the peak of regional metamorphism. The Décelles Batholith may project at depth underneath the Canadian Malartic deposit and could be associated with magmatic-hydrothermal mineralizing fluids in the Canadian Malartic deposit.

Gold mineralization at Canadian Malartic is spatially located on the contact of Phase 2 quartz-monzodiorite bodies. The proximity to the Cadillac Larder Lake Deformation Zone combined with the

* Corresponding author at: Western University, Earth Sciences, 1151 Richmond Street N, London, ON N6A 6B7, Canada.
E-mail address: sperrout@uwo.ca (S. Perrouty).

http://dx.doi.org/10.1016/j.oregeorev.2017.01.009
0169-1368/© 2017 Elsevier B.V. All rights reserved.

rheological contrast between steeply dipping clastic meta-sedimentary rocks and quartz-monzodiorite intrusions favored the protracted failure of the contacts between these two rock masses, thus forming favorable conduits for hydrothermal fluids (e.g., the Sladen Fault Zone). Such specific rheological behavior is demonstrated by domains of structural complexity, emphasized by the variance of the bedding dip. These structurally complex zones systematically host gold mineralization in the Canadian Malartic district of the Pontiac Subprovince proximal to the Cadillac Larder Lake Deformation Zone.

© 2017 Elsevier B.V. All rights reserved.

1. Introduction

The Abitibi Greenstone Belt and its abundant and diversified styles of gold deposits have been extensively investigated over the last century. Major mineralized systems consist of fault-hosted gold-bearing quartz – carbonate ± tourmaline vein deposits (Robert and Brown, 1986a,b; Neumayr et al., 2000; Olivo and Williams-Jones, 2002; Olivo et al., 2006; Dubé and Gosselin, 2007), intrusion-related deposits (Morasse et al., 1995; Robert, 2001; Helt et al., 2014) and volcanogenic massive sulfide deposits (Dubé et al., 2007; Mercier-Langevin et al., 2007). The Pontiac Subprovince, located south of the Abitibi Subprovince (Fig. 1), hosts the world-class intrusion-related Canadian Malartic gold deposit, where auriferous zones are spatially associated with felsic-intermediate intrusive bodies (Helt et al., 2014). Identifying the tectonic control on these intrusions and their timing relationship with respect to gold mineralization is critical to understanding metallogenic processes and may assist in targeting similar mineralized bodies in analogous tectonic settings.

This work integrates historical structural data collected in the Pontiac Subprovince with new observations made in the Canadian Malartic district, in order to elucidate the tectonic setting in which intrusive bodies and related gold mineralization were emplaced. We have achieved this by (1) revising the geological map by integrating airborne magnetic data with outcrop observations and previous data, (2) determining the relative timing and the structural controls on the emplacement of intrusive rocks and (3) comparing the spatial distribution of structurally complex zones with intrusive rock locations and gold mineralization.

2. Geological setting

The Archean Pontiac Subprovince includes over 2500 km^2 of Pontiac Group meta-sedimentary rocks (Fig. 1), which are mainly

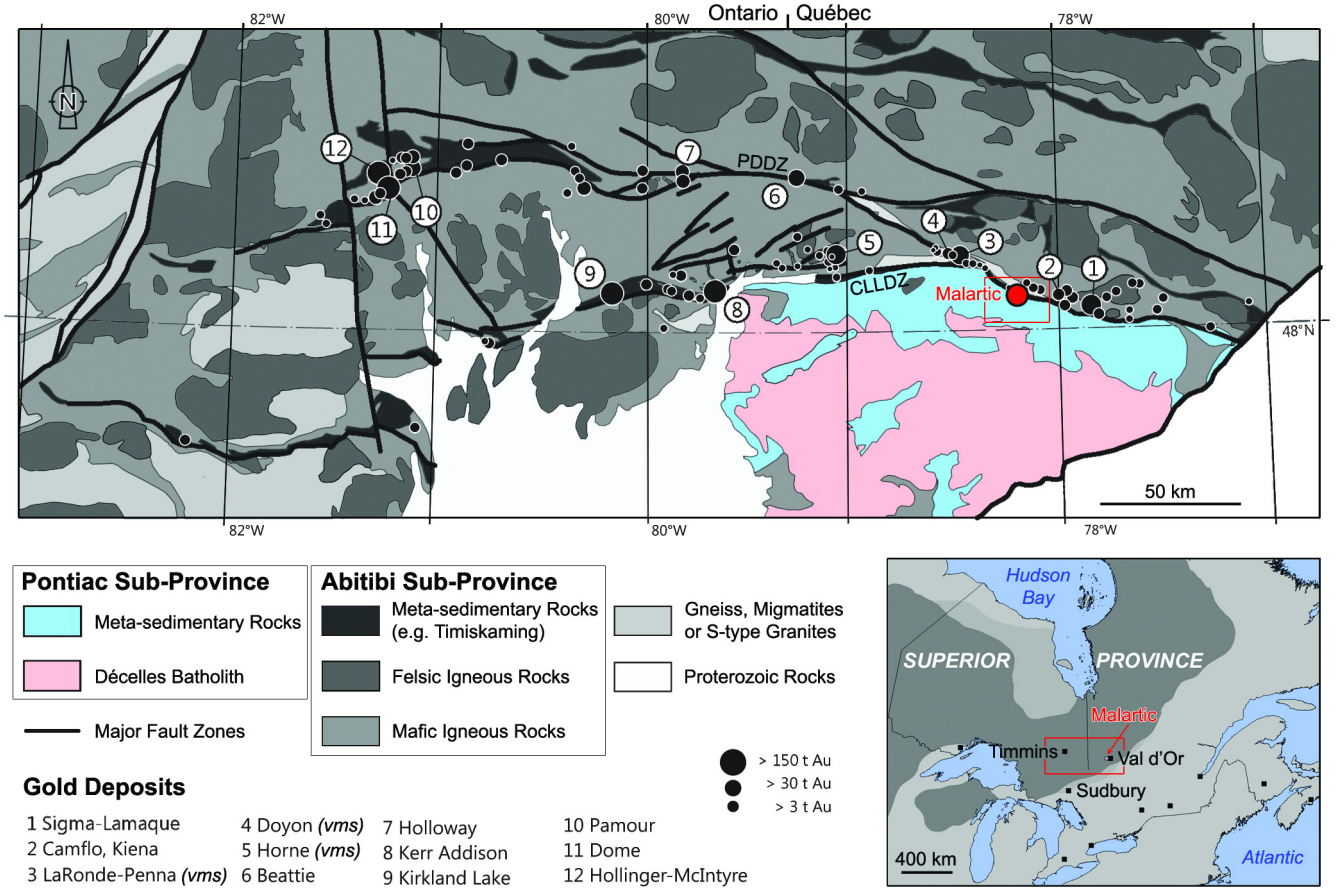

Fig. 1. Location of the Pontiac and Abitibi Subprovinces (modified after Robert and Poulsen, 1997). Gold deposits are primarily distributed along the Cadillac Larder Lake Deformation Zone (CLLDZ) and along the Porcupine Destor Deformation Zone (PDDZ). The world-class Canadian Malartic gold deposit is located on the north margin of the Pontiac Subprovince.

located south of the regional-scale Cadillac Larder Lake Deformation Zone (i.e., the Piché Group meta-volcanic and intrusive rocks, Pilote et al., 2000) and north of the Décelles Batholith (Rive et al., 1990; Mortensen and Card, 1993).

2.1. Lithologies

2.1.1. Meta-sedimentary rocks

The Pontiac Group comprises metamorphosed greywacke, siltstone, mudstone (±carbonaceous material) and rare conglomerate (with centimeter to millimeter size clasts of igneous and meta-sedimentary rocks) layers, which are interpreted as turbidite sequences (Camiré et al., 1993a; Mortensen and Card, 1993; Fallara et al., 2000). The detrital and metamorphic mineralogy consists mainly of quartz, plagioclase, biotite, white mica, chlorite and Fe-Ti oxide minerals. Garnet and staurolite occur with increasing metamorphic grade to the south, toward the Décelles Batholith. Rare observations of kyanite and sillimanite have also been reported in the southern and western parts of the Pontiac Subprovince (Jolly, 1980; Camiré et al., 1993a; Camiré and Burg, 1993; Benn et al., 1993; Powell et al., 1995). Hydrothermal alteration mineralogy in the footprint of the Canadian Malartic deposit and proximal to the Cadillac Larder Lake Deformation Zone include calcite, ferroan-dolomite, ankerite, microcline, albite, biotite, white mica, pyrite, rutile and ±epidote (Helt et al., 2014).

The provenance of the detrital material is poorly understood. Davis (2002) proposed that the igneous rocks from the Abitibi Subprovince are the main source of detrital zircons, based on the fact that most of the detrital and magmatic zircons have similar U-Pb ages distribution (i.e., 2685–2750 Ma) between the Pontiac and the Abitibi rocks. Davis (2002) however recognizes that older terranes may have also contributed, as suggested by the presence of detrital zircons that are older than the rocks currently exposed in the Abitibi Subprovince (i.e., >2750 Ma). By contrast, Card (1990) and Feng et al. (1992) proposed that the Pontiac Subprovince and the Abitibi Subprovince are unrelated blocks that were tectonically juxtaposed. Their model is supported by the presence of detrital zircon older than 2940 Ma (Gariépy et al., 1984), by lower εNd (Feng et al., 1993), lower Lu/Hf ratio in zircon (Stevenson and Patchett, 1990) and lower εHf in zircon (Corfu and Noble, 1992) in the Pontiac meta-sedimentary rocks compared with the Abitibi igneous and meta-sedimentary rocks. Furthermore, whole rock lithogeochemical interpretation by Camiré et al. (1993a) revealed that the modeled Pontiac meta-sedimentary rock source is not consistent with the composition of outcropping granitoids, komatiites and tholeiitic basalts in the Abitibi Subprovince.

The maximum deposition age for the Pontiac Group sediments is constrained by the youngest detrital zircon grain U-Pb age at 2685.3 ± 3.0 Ma (within a population of 54 grains, Davis, 2002) and 2682.7 ± 1.9 Ma (within a population of 3 grains, Mortensen

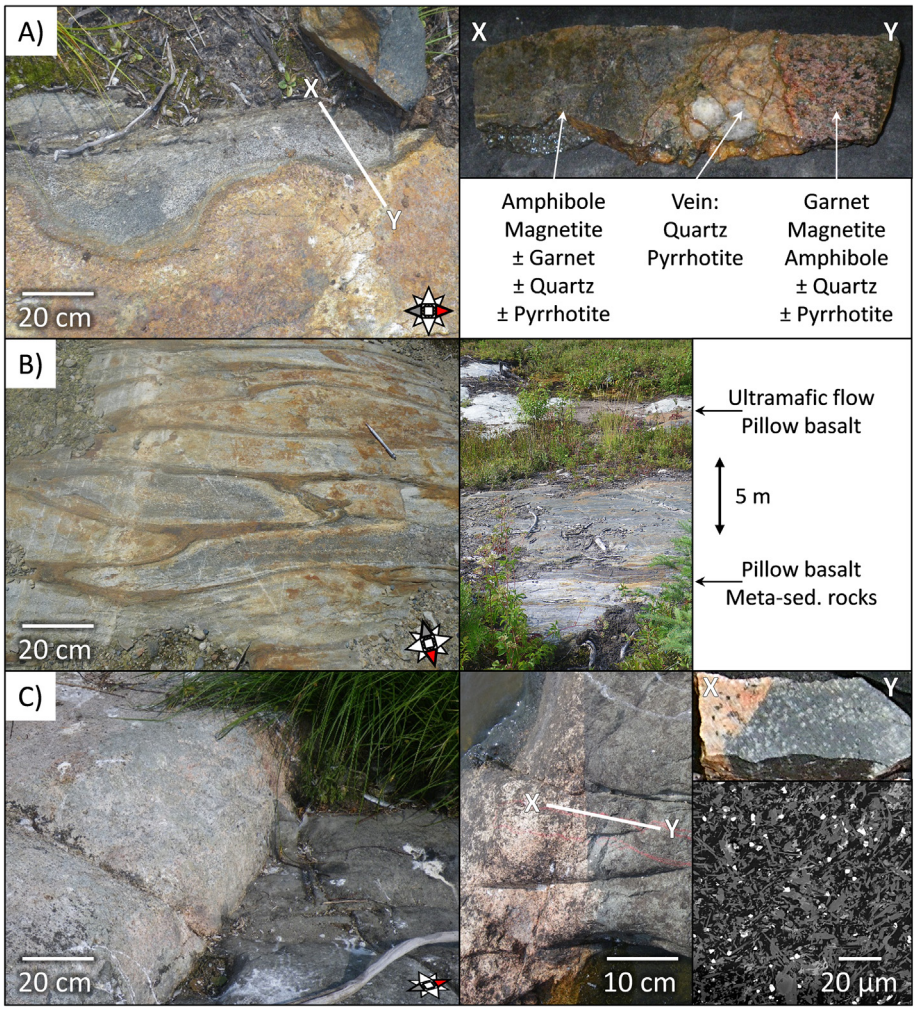

Fig. 2. Example of iron-formations, meta-volcanic rocks and diabase dykes in the Pontiac Subprovince. Location are indicated in Fig. 4. A) Iron-formations in the Pontiac Group consist of amphibole-rich and garnet-rich rock-types. Quartz-pyrrhotite veins are frequent. B) meta-volcanic rocks correspond to pillow basalt and mafic–ultramafic flows interlayered with meta-sedimentary rocks. C) Diabase dykes (here within the Lac Fournière pluton) have sharp contact with their host rock and display augite phenocrysts in a fine grained ground mass.

and Card, 1993). The minimum deposition age is estimated based on the magmatic zircon crystallization U-Pb ages of felsic-intermediate intrusions that were emplaced into the Pontiac Group at 2682.4 ± 1.0 Ma (Lac Fournière pluton; Davis, 2002) and 2681.0 ± 1.9 Ma (Lac Fréchette pluton, Mortensen and Card, 1993).

2.1.2. Iron formations

Iron formations in the Pontiac Group were briefly reported by Desrochers and Hubert (1996) and Fallara et al. (2000) as small magnetite-rich bands. In this study we identified two major rock types: iron-rich amphibolite and iron-rich garnetite (Fig. 2A). They both display similar mineralogy with variable proportion of garnet (>50% in the garnetite), amphibole (e.g., grunerite, cummingtonite, ±hornblende), magnetite, ±quartz and ±pyrrhotite. Whole rock XRF analysis reveals total iron contents (as Fe_2O_3) of up to 62 wt.%.

2.1.3. Meta-volcanic rocks

Meta-volcanic rocks in the Pontiac Group correspond to successive layers of mafic-ultramafic flows and pillow-lavas (Camiré et al., 1993b; Fallara et al., 2000), which are parallel to the bedding of their host meta-sedimentary rocks (Fig. 2B). Their thickness varies between 100 and 500 m and their mineralogy consists mainly of chlorite, amphibole, ±plagioclase, ±quartz, magnetite and ilmenite.

Camiré et al. (1993b) interpreted interlayered meta-volcanic rocks within the Pontiac Group as allochthonous slices that were

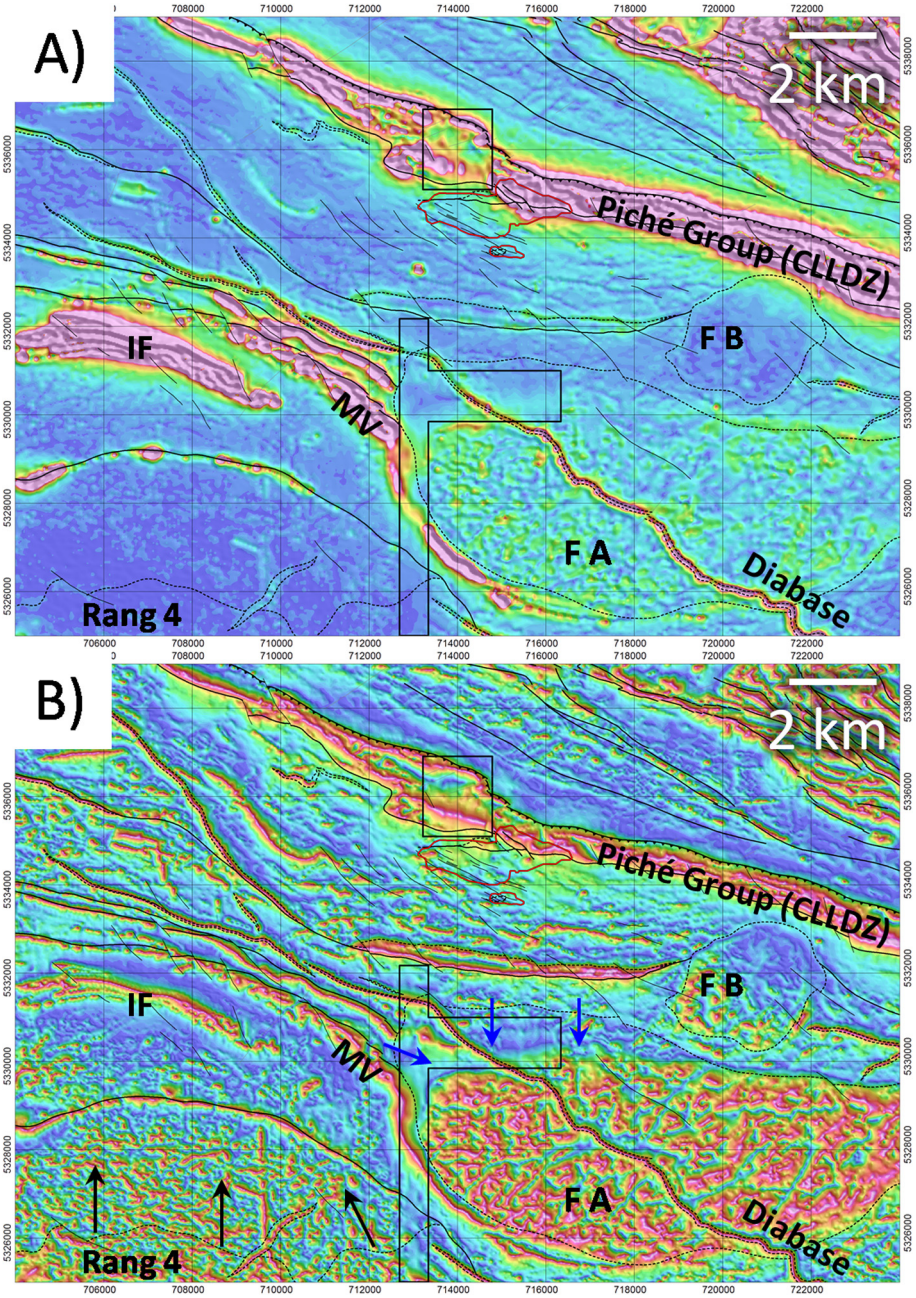

Fig. 3. Processed maps of the 2012 airborne magnetic survey (D'Amours and Intissar, 2012). The coordinate system is NAD83-UTM17N. The red line represents the open-pit mine (as designed in 2013). CLLDZ: Cadillac Larder Lake Deformation Zone. A) Analytic signal map. Main magnetic bodies are indicated: IF, iron-formation, MV, meta-volcanic rocks. The outline areas are of poorer quality because of higher ground clearance at the town of Malartic and the Lac Mourier road. B) Tilt derivative map. The arrows indicate a south-dipping contact between the Lac Fournière A and B plutons (FA, FB) and the meta-sedimentary rocks (blue arrows), and a north-dipping contact between the Rang 4 pluton and the meta-sedimentary rocks (black arrows). Magnetic map texture suggests that the Rang 4 pluton extends at relatively shallow depth several kilometers north of its outcropping locations. (For interpretation of the references to color in this figure legend, the reader is referred to the web version of this article.)

tectonically emplaced during the first phase of deformation. Dimroth et al. (1983) similarly proposed that the meta-volcanic rocks represent fragments of the Pontiac Group basement. However, in this study we observed meta-sedimentary rocks underlying and overlaying the pillow-lavas (Fig. 2B) without any evidence of a fault zone at the contact, suggesting that these volcanic rocks were likely extruded during sedimentation.

2.1.4. Felsic-intermediate intrusions

Felsic-intermediate intrusive rocks in the Pontiac Subprovince south of the Canadian Malartic deposit define three main suites represented by the Lac Fournière plutons, the Sladen intrusions and the Décelles Batholith.

The Lac Fournière plutons are the oldest known intrusions in the Pontiac Subprovince, dated at 2682.4 ± 1.0 Ma (U-Pb on zircon, Davis, 2002). The mineralogy of these monzodiorites comprises plagioclase, hornblende, ±biotite, ±quartz, ±white mica, ±K-feldspar (Rive et al., 1990; Fallara et al., 2000). The main pluton is over 10 km long and 6 km wide (Figs. 3 and 4). Mafic xenoliths are commonly observed.

The Sladen intrusions consist of quartz-monzodiorites and granodiorite (Helt et al., 2014; De Souza et al., 2015, 2016) that are

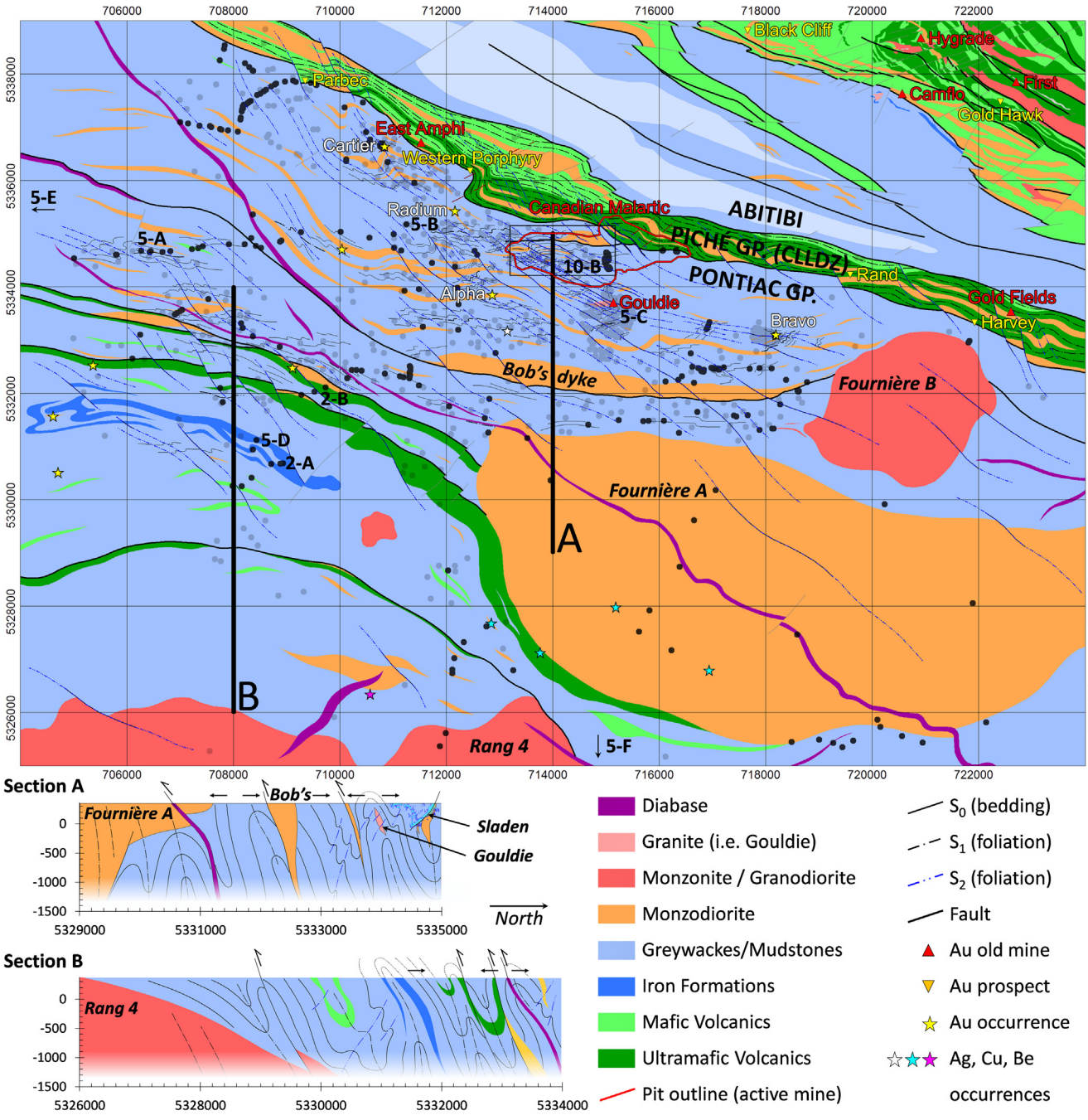

Fig. 4. Revised map of the Pontiac Subprovince, south of the Canadian Malartic deposit (modified after Derry, 1939; Gunning and Ambrose, 1940, Minerais Lac Limited, unpublished reports and maps, Sansfaçon et al., 1987; Fallara et al., 2000, Ministère des Ressources Naturelles du Québec, SIGEOM Database, 2016, http://sigeom.mines.gouv.qc.ca/ and Canadian Malartic Exploration, 2012, unpublished datasets). Historical gold mines, prospects, occurrences and field photographs (from Fig. 2 and 5) are located. Black and grey points represent field structural observations from this study and from previous works. The coordinate system is NAD83-UTM17N. The red line represents the open-pit mine (as designed in 2013). CLLDZ: Cadillac Larder Lake Deformation Zone. F_1 fold locations on the schematic cross-sections are mainly interpreted from opposing younging directions (arrows). (For interpretation of the references to color in this figure legend, the reader is referred to the web version of this article.)

composed of plagioclase, K-feldspar, quartz, ±biotite, ±chlorite, ±white mica, ±epidote and ±Fe-Ti oxide minerals (Derry, 1939; Fallara et al., 2000). Because of a strong potassic and silica hydrothermal alteration they were previously described as quartz-syenites (e.g., Gunning and Ambrose, 1940; Sansfaçon et al., 1987). The Sladen intrusions define a network of east-west-elongated, south-dipping bodies, that are either plunging gently to the west or steeply to the east in a nearly orthogonal pattern (as schematized by Fallara et al., 2000). Their age is estimated to be around 2676–2679 Ma (U-Pb on zircon and titanite, Helt et al., 2014; De Souza et al., 2015, 2016).

The Décelles Batholith (Fig. 1) consists of multiple S-type monzogranites and pegmatites (Rive et al., 1990; Feng et al., 1993), which contain variable amounts of quartz, plagioclase, K-feldspar, biotite and white mica. meta-sedimentary and mafic xenoliths are commonly observed. Garnet and sillimanite have been reported in the marginal zones (Rive et al., 1990). The Décelles magmatism is considered to be syn- to late- tectonic (Rive et al., 1990) and to be derived from partial melting of the Pontiac meta-sedimentary rocks at depth in response of crustal thickening (Feng and Kerrich, 1991, 1992; Chown et al., 2002). U-Pb monazite ages indicate a lower limit for the crystallization age of the Décelles Batholith, ca. 2663–2668 Ma (Mortensen and Card, 1993).

2.1.5. Meta-basic dykes

Meta-basic dykes are common in the Pontiac Subprovince. They are 0.05–2 m thick (with significant boudinage) and their orientation varies between E-W and NW-SE. Xenoliths of granitoids and of meta-sedimentary rocks are locally observed. These dykes were first reported by Derry (1939) and were interpreted as lamprophyre-equivalent by Camiré et al. (1993b) and De Souza et al. (2016). The major minerals are amphibole (mainly hornblende, rare anthophyllite) and ±plagioclase (anorthite). Biotite, quartz, calcite and pyrite are present as hydrothermal alteration products in the footprint of the Canadian Malartic deposit (Sansfaçon et al., 1987; Fallara et al., 2000) and the mineral relative abundance progressively decreases with increasing distance from the deposit (Perrouty et al., 2015).

Derry (1939), Sansfaçon et al. (1987) and De Souza et al. (2016) reported that the meta-basic dykes crosscut the Sladen intrusions in the Canadian Malartic deposit. Similar dykes (referred to as "lamprophyres") from the Abitibi Subprovince, which may be considered as the equivalent of the meta-basic dykes of the Pontiac Subprovince, have been dated at 2674 ± 2 Ma (U-Pb on titanite, Wyman and Kerrich, 1993).

2.1.6. Diabase dykes

Diabase dykes cross-cut both the Pontiac and the Abitibi Subprovinces and are clearly visible in airborne magnetic maps (Fig. 3). According to field observations, these 10–20 m thick dykes have sharp contacts with their host rock (Fig. 2C). They are composed of augite phenocrysts (mm size) in a fine grain (<10 μm) groundmass with pyroxene, albite, magnetite and titanite (Fig. 2C).

Based on their orientation, two dyke swarms can be identified: a main NW-SE trending swarm which may belong to the Sudbury swarm (~1200 Ma, Ernst, 1994; Buchan and Ernst, 2004) and a secondary NE-SW trending swarm which may belong either to the Abitibi swarm (~1100 Ma, Ernst and Buchan, 1993) or to the Biscotasing and Senneterre swarms (~2200 Ma, Buchan et al., 1993).

2.2. Structures and geodynamic model

The first structural study of the Canadian Malartic district was published by Derry (1939). Subsequent studies completed the structural model and reached similar interpretations in the north-western part of the Pontiac Subprovince (Sansfaçon et al., 1987; Camiré and Burg, 1993; Benn et al., 1993; Desrochers and Hubert, 1996; Fallara et al., 2000; De Souza et al., 2015, 2016). Three main deformation events have been interpreted:

D_1 is considered to be a major isoclinal folding event in the Canadian Malartic region despite the fact that structural features (e.g., fold hinges, foliation) are rarely seen (Derry, 1939). Opposing younging directions of bedding are the main indicator of the F_1 folding. The S_1 pressure-solution cleavage is assumed to be mainly sub-parallel to the bedding and is observed as a folded fabric in F_2 fold hinges (De Souza et al., 2015, 2016). Abundant observations of D_1-related structures in the north-western part of the Pontiac Subprovince are presented by Camiré and Burg (1993).

D_2 created abundant open to closed F_2 folds as well as the NW-SE-trending S_2 biotite foliation (Fig. 5). South-west of the Canadian Malartic deposit, a major F_2 drag-fold associated with several NW-SE high-strain zones was described by Derry (1939). These NW-SE zones correspond to alternating high and low strain S_2-parallel bands almost perpendicular to the F_2-folded bedding (De Souza et al., 2015). They are interpreted to be located within a major S-shaped F_2 fold hinge zone (De Souza et al., 2016). F_2 fold axes plunge 60 degrees to the East, coaxial with the L_2 stretching lineation (Sansfaçon et al., 1987; Sansfaçon and Hubert, 1990).

D_3 is a late deformation event associated with conjugate kinks and with a non-penetrative NE-SW-trending crenulation cleavage (Sansfaçon and Hubert, 1990; Desrochers and Hubert, 1996). F_3 open folds are rare and mainly interpreted from subtle changes in the orientation of the S_2 foliation at the outcrop scale (e.g., Cartier zone, Neumayr et al., 2000; Blacklock, 2015).

These shortening events correlate with those described in the Cadillac Larder Lake Deformation Zone (i.e., in the Piché Group, Pilote et al., 2000; Lafrance, 2015; Bedeaux et al., 2017), in meta-sedimentary rocks north of this major crustal break. (i.e., the Cadillac Group, Bedeaux, 2012) and in meta-volcanic rocks of the southern Abitibi volcanic zone (Daigneault et al., 2002). The principal foliation in the Piché Group (Fig. 4) is referred to S_1 by Pilote et al. (2000), Daigneault et al. (2002), Bedeaux (2012) and Bedeaux et al. (2017) or to S_2 by Lafrance (2015). In the Canadian Malartic area, it likely corresponds to the S_1 fabric of the Pontiac meta-sedimentary rocks (Fig. 4). It is overprinted by a NW-SE-trending steeply dipping foliation associated with S-shaped folds in the Pontiac Group (D_2 event of Derry, 1939 and De Souza et al., 2017), which correlates with similar features observed in the Cadillac Group (Bedeaux, 2012) and in some segments of the Cadillac Larder Lake Deformation Zone (D_3 event of Bedeaux et al., 2017). The subsequent deformation event generated a series of Z-shaped folds and a NE-SW-trending crenulation cleavage in the meta-volcanic and meta-sedimentary rocks of the Abitibi Subprovince, which is referred to S_2 by Pilote et al. (2000) and Daigneault et al. (2002), to S_3 by Lafrance (2015) or to S_4 by Bedeaux et al. (2017). It is also observed in the Pontiac Subprovince and considered to be a minor D_3 event (Desrochers and Hubert, 1996). Daigneault et al. (2002), Bedeaux (2012), Lafrance (2015), and Bedeaux et al. (2017) interpreted D_3 structures to be caused by late dextral transcurrent movement along the Cadillac Larder Lake Deformation Zone.

Current geodynamic models for the Pontiac and the Abitibi Subprovinces imply an overall north dipping subduction setting (Daigneault et al., 2002; Wyman et al., 2002). The Pontiac Subprovince is interpreted as a foreland basin (Davis, 2002), as an accretionary prism (Card, 1990; Daigneault et al., 2002), or as an allochthonous terrane that was accreted against the Abitibi Subprovince (Feng et al., 1992). These models are primarily based on zircon age determination or lithogeochemical analyses of meta-sedimentary and intrusive rocks. They are nevertheless consistent with north-dipping major structures in the Pontiac Subprovince,

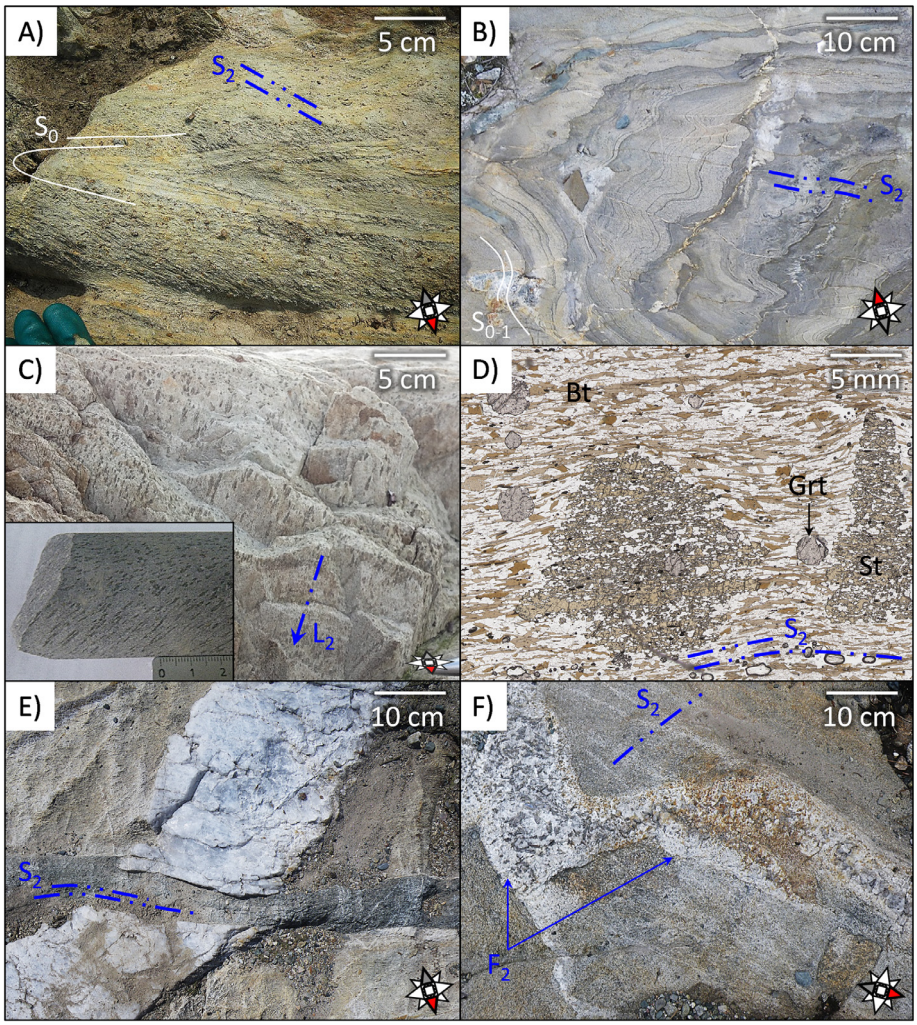

Fig. 5. Interpreted field photographs of major structures. Location are indicated on Fig. 4. A) Tight F_1 fold without visible axial planar foliation. The main foliation (S_2) cuts both limb of the fold that is interpreted as F_1. B) Typical F_2 closed fold hinge with an S_2 axial surface marked by biotite alignment and parallel quartz-filled fractures. C) Micas, quartz and ±calcite mm-scale pseudomorphs marking an L_2 stretching lineation steeply plunging toward the east. The inset show similar pseudomorphs on a piece of drill-core. D) Staurolite (St) poikiloblast overprinting the S_2 biotite (Bt) foliation in the Pontiac meta-sedimentary rocks. Garnet (Grt) are also present. E) Early D_2 west-dipping gold-barren quartz vein cross-cut by a meta-basic dyke and by the S_2 foliation. F) Open F_2 folding of a granitic dyke linked to the Décelle batholith. Note the subtle chilled margin along the contact with the meta-sedimentary host rock.

which have been interpreted from the Lithoprobe seismic reflection profile, south of Rouyn-Noranda (Benn et al., 1993).

2.3. Mineral occurrences

Gold is the main commodity in the studied area (Fig. 4). Several small deposits were historically mined within the Piché Group meta-volcanic and intrusive rocks. The only known world-class gold system in the Pontiac Subprovince is the Canadian Malartic deposit, located 30 km west of Val d'Or (Fig. 1). It is a low-grade, large-tonnage deposit with a gold endowment exceeding 18.6 million ounces (10.8 Moz of measured and indicated resources + 1.1 Moz of inferred resources + 1.2 Moz of Osisko production + 5.5 Moz of historical production Gervais et al., 2014).

Mineralization in the Canadian Malartic deposit is localized primarily along two principal structural trends: an E-W-oriented steeply south-dipping Sladen Fault Zone and NW-SE S_2-parallel bands, south of the Sladen Fault (Derry, 1939). Gold is mainly associated with pyrite (Helt et al., 2014). The potassic, silicic and carbonate alteration of the meta-sedimentary rocks and of felsic-intermediate intrusive rocks were well described by Derry (1939), Helt et al. (2014) and De Souza et al. (2015, 2016) and form biotite, K-feldspar, albite (in the meta-sedimentary rocks), white mica, quartz (silicification in the intrusive rocks), calcite, ±ferroan-dolomite, ±ankerite, rutile, ±hematite and ±epidote. Mass gains in Au, Ag, Te, Bi, Mo, Pb, Sb, and W have been documented by Helt et al. (2014) and De Souza et al. (2015, 2016).

Hydrogen and oxygen isotopic composition of biotite, hematite and quartz, and whole rock alteration assemblages led Helt et al. (2014) to propose mineralizing fluids of magmatic origin, although their interpretation has been challenged by Beaudoin and Raskevicius (2014), who suggested metamorphic fluid origin. De Souza et al. (2016) considered two phases of gold mineralization: an early magmatic-hydrothermal event and a main hydrothermal event sharing similarities with typical orogenic gold systems. They interpreted the latter as *syn*-D_2, based on the structural relationship between the mineralized veins and the D_2 structures. The absolute timing of this event is estimated at 2664 ± 11 Ma (re-Os on molybdenite, De Souza et al., 2016).

Other commodity occurrences in the Pontiac Subprovince include silver (associated with quartz – pyrite – galena veins in greywacke, Banas and Melchiorre, 1998), copper (associated with

quartz – chalcopyrite – bornite veins, south-west of the Lac Fournière plutons, Gagnier, 1997) and beryl (associated with quartz – biotite – tourmaline – molybdenite veins in a pegmatite dyke at the margin of the Décelles Batholith, Bérubé, 1962).

3. Geological and geophysical mapping

3.1. Airborne geophysical data

Airborne geophysical surveys were used to support geological and structural mapping work. Such surveys help delineate geological units, identify major structural features and interpret their kinematics and 3D geometries (Betts et al., 2003, 2007; Perrouty et al., 2012, 2014). Available airborne geophysical datasets in the Canadian Malartic district consist of two regional aeromagnetic surveys, conducted in 1994 and 2012 by the Ministère des Ressources Naturelles du Québec (Dion and Lefebvre, 1997; D'Amours and Intissar, 2012), and of a local aeromagnetic-EM-radiometric survey conducted in 2006 by Canadian Malartic Exploration (formerly Osisko Exploration). In this work, we predominantly used the regional helicopter-borne magnetic survey conducted in 2012, because it provides the highest resolution data and the best coverage. Survey parameters are: a N-S line spacing of 100 m, a E-W tie-line spacing of 1000 m and an elevation of 40 m. The airborne magnetic data were not considered to help interpreting surface geology directly over the town of Malartic because of the higher required ground clearance (300 m) and the presence of anthropogenic signals. Data processing was performed using Geosoft Oasis Montaj software (http://www.geosoft.com/). A series of maps were produced to guide geological interpretations. Processing methods include reduction to the magnetic pole, analytic signal (Fig. 3A) (MacLeod et al., 1993), first vertical derivative using amplitude normalization (automatic gain control, Rajagopalan and Milligan, 1994) and tilt derivative (Fig. 3B) (Verduzco et al., 2004).

3.2. Revised regional mapping

Over 7900 historical drill holes and outcrop observations by Derry (1939), Gunning and Ambrose (1940), Minerais Lac Limited (unpublished reports and maps), Sansfaçon et al. (1987), Fallara et al. (2000), Ministère des Ressources Naturelles du Québec (SIGEOM Database, 2016, http://sigeom.mines.gouv.qc.ca/) and Canadian Malartic Exploration (formerly Osisko Exploration, 2012, unpublished datasets) were integrated with 400 new field observations and airborne magnetic maps to produce a revised geological map of the area (Fig. 4).

3.2.1. Highly magnetic units

A significant enhancement of older maps resides in the definition of highly magnetic bodies such as the iron formations and ultramafic units. Iron formations exhibit the strongest magnetic susceptibility (over 1 SI, based on field measurements using a KT 10 magnetic susceptibility meter) and the strongest magnetic remanence (over 10 A/m, laboratory measurement, method of Enkin et al., 2012) in the Pontiac Subprovince. They are only observed in the south-west portion of the mapped area (Fig. 4), where positive magnetic anomalies highlight at least two distinct regional-scale fold generations (Fig. 3B). The first fold generation (F_1) is almost isoclinal with an axial surface oriented E-W. A major F_1 antiform fold hinge limits the extent of the iron formations toward the west. The second fold generation (F_2) is asymmetric, open to tight and its axial surface is oriented NW-SE, parallel to the regional S_2 foliation. The overall open-crescent-shaped and doubly-plunging anticlinal fold geometry of the iron formations results of interference between F_1 and F_2 fold hinges (Fig. 4).

Mafic-ultramafic rocks in the study area consist mainly of three sub-parallel 100–500 m thick layers (Fig. 4). The variable thickness and the discrete distribution of positive magnetic anomalies (Fig. 3A) indicate a significant boudinage of these layers. Interpretation of the magnetic maps suggests that the ultramafic layers are truncated on their east side by the Lac Fournière plutons (Fig. 3), however cross-cutting evidences were not observed in the field.

3.2.2. Major intrusions

Airborne magnetic data helps identify and refine the shape of large intrusive bodies. Four main intrusions are recognized in the Malartic district: Bob's dyke, Lac Fournière A, Lac Fournière B and Rang 4 (Fig. 4). Their composition was determined from field and petrological observations (21 polished thin-sections). Magnetic lineaments transecting each of these intrusions correspond to a subtle structural fabric observed on outcrops and are aligned along the S_0-S_1 fabric in the meta-sedimentary host rocks. Therefore, these intrusions are interpreted to be early- to *syn*-D_1.

Bob's dyke is an E-W elongated quartz-monzodiorite body located 2 km south of the Canadian Malartic deposit. It is composed mainly of plagioclase, biotite, ±quartz, ±K-feldspar, ±hornblende. Sulfide minerals (pyrite and/or pyrrhotite) with no associated gold mineralization are locally abundant within Bob's dyke. Its northern and southern margins are moderately magnetic ($\sim 5 * 10^{-3}$ SI).

The Lac Fournière A and B intrusions were previously mapped as a single body named "Lac Fournière Pluton". Mineralogical and magnetic signatures indicate at least two distinctive bodies that are separated by a thin band of garnet- and staurolite- bearing meta-sedimentary rocks. The Lac Fournière A is a moderately magnetic ($\sim 16 * 10^{-3}$ SI) monzodiorite pluton composed mainly of plagioclase, hornblende, ±biotite, ±quartz, ±K-feldspar. The three-dimensional geometry of this intrusion can be estimated by comparing intensity and texture on the aeromagnetic maps with field outcrop and drill hole information. Its texture is characterized by short-wavelengths variations of an overall positive magnetic response (Fig. 3). The lower amplitude of these variations in the northern part of the pluton suggests a south-dipping contact with the host meta-sedimentary rocks. Thickening of the pluton toward the south correlates with higher magnetic signal. The Lac Fournière B is a weakly magnetic ($\sim 0.5 * 10^{-3}$ SI) granodiorite pluton composed mainly of quartz, K-feldspar, plagioclase, white mica, ±biotite, ±hornblende. The contacts between these intrusions and their meta-sedimentary host rocks were not observed in the field.

The Rang 4 pluton is a weakly magnetic ($\sim 0.4 * 10^{-3}$ SI) quartz-monzonite body composed of hornblende, K-feldspar, plagioclase, ±quartz, ±biotite, ±white mica. Its relationship with the Décelles Batholith is unknown. Its magnetic texture shows short-wavelengths variations. Subtle increase of the wavelengths and lower amplitude of the variations suggest that this intrusion extends to the north at shallow depths underneath the meta-sedimentary rocks for more than 4 km (Figs. 3B, 4 section B).

3.3. Compilation of field structural data

Historical structural data in the Canadian Malartic district consists of more than 1700 orientation measurements of bedding, foliations, lineations and fold axes that were acquired by Gunning and Ambrose (1940), Minerais Lac Limited (unpublished maps), Sansfaçon et al. (1987), and Ministère des Ressources Naturelles du Québec (SIGEOM Database, 2016, http://sigeom.mines.gouv.qc.ca/). They were evaluated and augmented with 590 new field structural data points. Bedding, foliation and lineation data are displayed on Fig. 6 using maps and stereoplots.

The use of interpolated grids to display strike and dip allows for a better visualization of the overall regional trends when working with large structural datasets. However, each of the structural "anomalies" must be systematically evaluated by scrutinizing each data point before interpretation (e.g., an apparent "anomaly" of strike may be caused by sub-horizontal measurements). Interpolated grids were produced using the minimum curvature (Briggs, 1974) option of Geosoft Oasis Montaj software

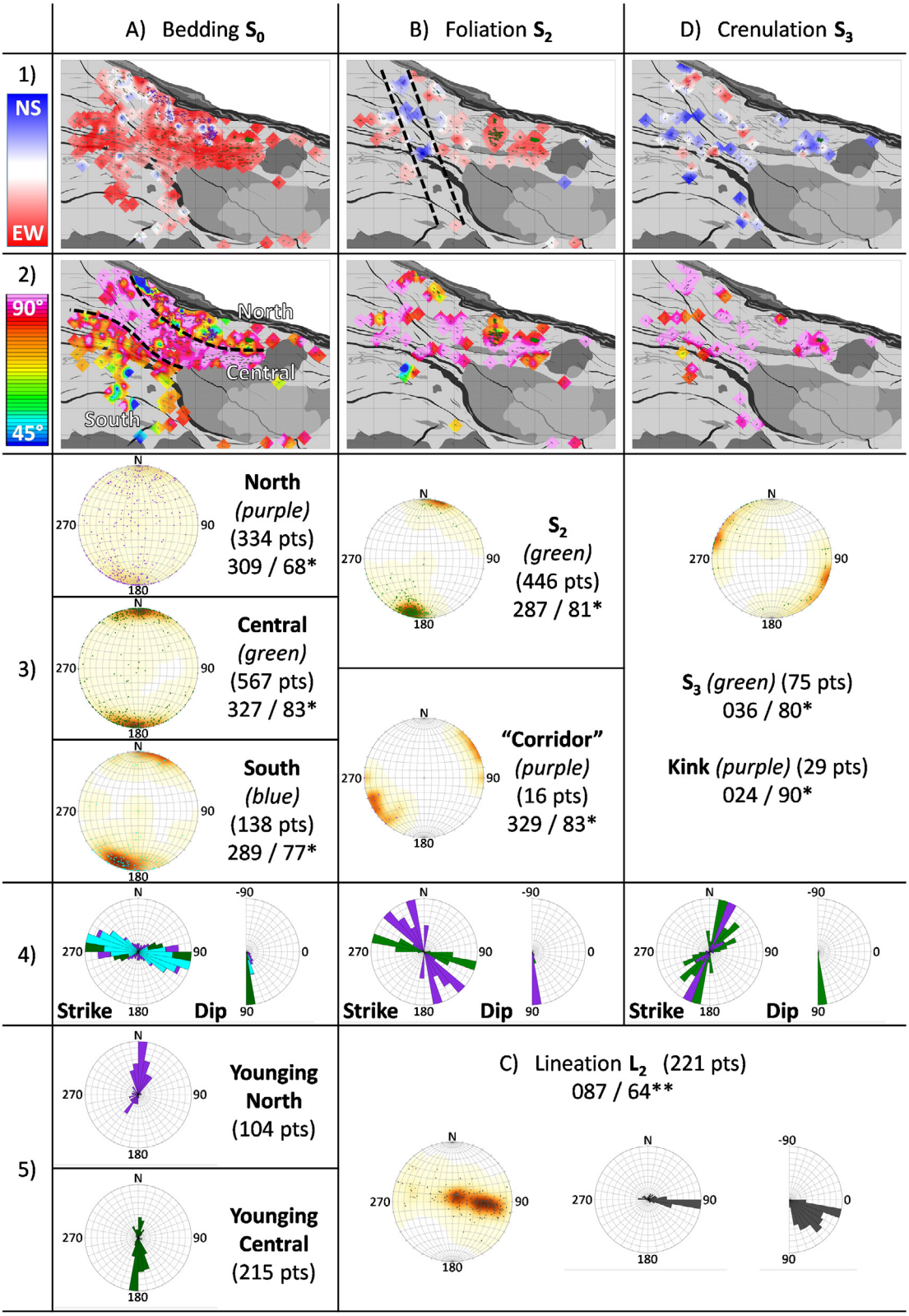

Fig. 6. Compilation of structural datasets from Gunning and Ambrose (1940), Minerais Lac Limited (unpublished reports and maps), Ministère des Ressources Naturelles du Québec (SIGEOM Database, 2016, http://sigeom.mines.gouv.qc.ca/) and this study. See text for details. *Strike and Dip, right-hand rules. **Direction and Plunge.

(http://www.geosoft.com/). Stereoplot (Schmidt diagrams – lower hemisphere) and rose diagrams (Fig. 6) complement and validate the interpretation of interpolated grids. They were produced using GOCAD 14.1 software (Paradigm, http://www.pdgm.com/, Mira Geosciences, http://www.mirageoscience.com/).

3.3.1. Bedding

Bedding orientations in meta-sedimentary rocks constitute the largest structural dataset with over 1000 historical and new measurements. Interpretation of interpolated grids of bedding orientations, stereoplots and field observations revealed three structural domains: North, Central and South (Fig. 6-A).

The North domain is restricted to the vicinity of the Canadian Malartic deposit. Compilation of 334 strike and dip measurements shows a heterogeneous distribution, which results from interference between F_1 and F_2 fold generations. Sub-horizontal bedding (with younging upward) is principally observed at the Cartier, Radium, Alpha, Gouldie and Bravo gold mineralized zones (see Fig. 4 for location), where macro-scale F_1 and F_2 fold hinges coincide.

The Central domain corresponds to a high strain D_1 corridor around Bob's dyke and in the north-west part of the mapped area. It has a homogeneous distribution of bedding orientations: 567 strike and dip measurements display an average WNW-ESE strike and a sub-vertical dip. Such high strain may have been caused by the buttressing effect of the Lac Fournière pluton.

The South domain is located south of the meta-volcanic layers and south of the Lac Fournière plutons. The average of 138 bedding measurements suggests an overall steeply north-dipping WNW-ESE orientation. F_1 and F_2 fold hinges are rarely seen on outcrops in the South domain but are obvious on aeromagnetic maps (e.g., in the iron formations, Fig. 3).

3.3.2. Variance of the bedding dip

In order to map the spatial distribution of the structurally complex zones (e.g., fold interference zones), the variance of the bedding dip has been calculated by following the variance formula as follows: $\frac{1}{N}\sum_i^N (x_i - \bar{x})^2$. This was accomplished in steps (using Geosoft Oasis Montaj software, http://www.geosoft.com/) by kriging the bedding dip data twice to produce (1) a fine grid with cell size of 100 m and (2) a coarser grid of cell size 300 m. The coarse grid was resampled to a 100 m resolution grid then subtracted from the fine grid to produce a difference grid with a spatial resolution of 100 m. This difference grid was subsequently squared and the resultant grid was re-gridded at 300 m by averaging the data within windows of 3 * 3 cells. The individual cells of this final grid (Fig. 7) represent the results of the variance operation as outlined in the above equation. The map of the bedding dip variance (Fig. 7) remarkably illustrates the three structural domains and the

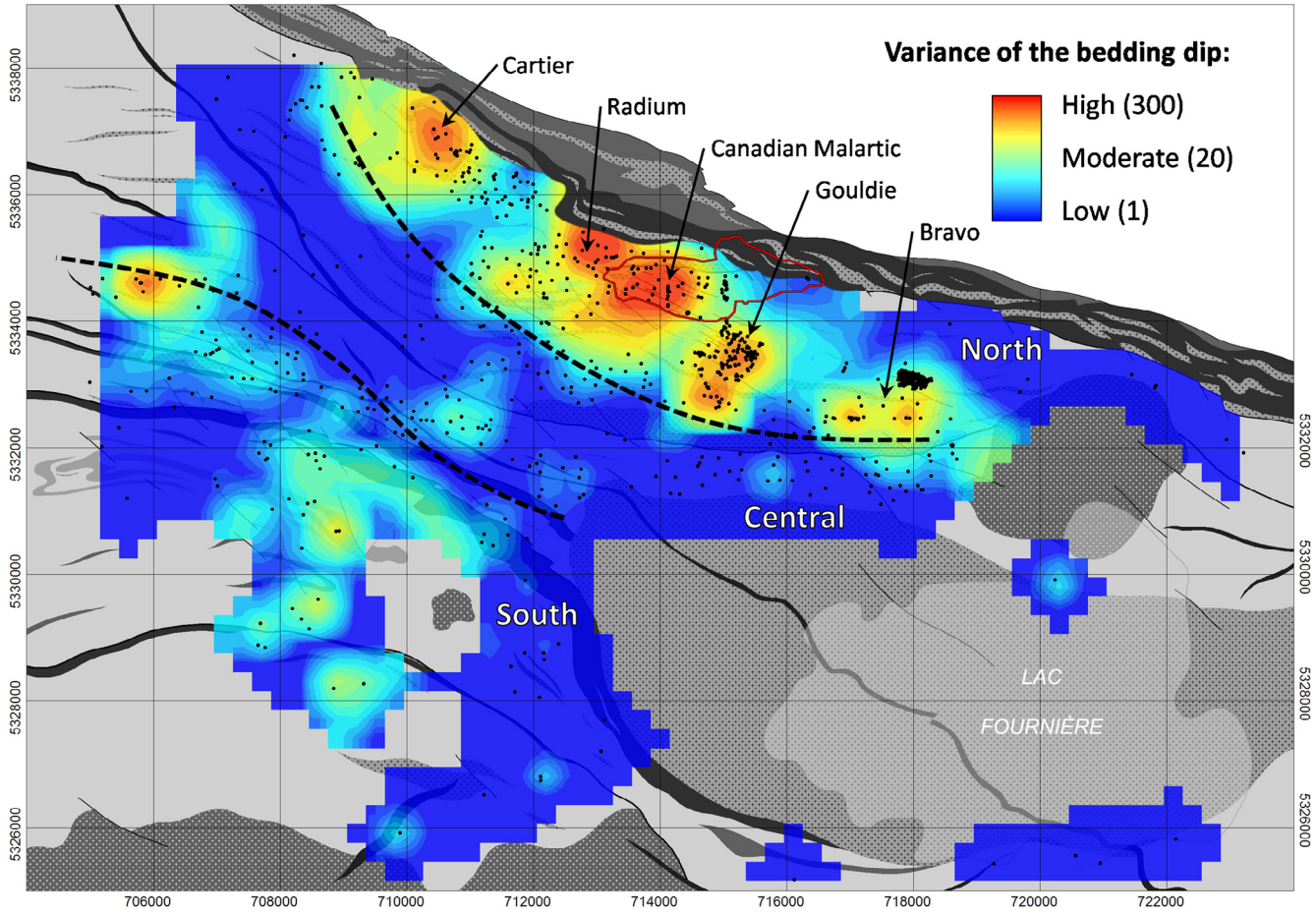

Fig. 7. Map of the variance of the bedding dip. See text for the calculation method. The coordinate system is NAD83-UTM17N. The red line represents the open-pit mine (as designed in 2013). Black dots represent input data points. Three major structural domain, North, Central and South, can be interpreted. High variance anomalies in the North domain are systematically correlated with mineralized areas (i.e., Cartier, Radium, Canadian Malartic, Gouldie and Bravo zones).

structurally complex zones (i.e., high variance zones), which appear to be systematically correlated with gold occurrences.

3.3.3. Younging directions

Over 300 younging directions were measured from graded-bedding, cross-bedding or load-cast markers, and were distributed homogeneously over the entire area to limit the bias induced by sample location. Each bedding data point is not systematically associated with a younging direction due to the lack of an obvious marker at some locations and younging directions are rarely reported in historical datasets. In this study, younging directions were preferentially measured in F_2 fold hinges in order to discriminate F_1 and F_2 fold influence.

Younging direction in the North domain (i.e., in the vicinity of the Canadian Malartic deposit) is dominantly toward the north (104 measurements, Fig. 6-A5), whereas younging direction in the Central domain is dominantly toward the south (215 measurements, Fig. 6-A5). No dominant direction can be determined for the South domain, where only three younging observations are reported. The alternation of north and south polarities at various scales (from outcrop to domains) is attributed to F_1 isoclinal folds, with small meter-scale folds visible on rare outcrops (e.g., Fig. 5-A), intermediate-scale folds interpreted from opposing younging directions and a large regional-scale antiform fold interpreted from overall trends in younging direction between the North and the Central structural domains.

3.3.4. Folds, foliations, lineation and kinks

The S_1 foliation is rarely observed on outcrop, even in hinges of F_1 folds (Fig. 5-A) where it should mark the axial surface. A faint pressure solution cleavage and a subtle biotite-white mica alignment in microlithons have been locally seen in thin-section and are interpreted as relic S_1 fabric. Tight to isoclinal F_1 fold hinges (Fig. 5-A) are rarely found and F_1 folds are generally interpreted on the basis of opposing younging directions of bedding.

The S_2 foliation is the main structural fabric in the area and it defines the axial surface of meter-scale open to tight steeply dipping F_2 folds (Fig. 5-B). F_2 folds are frequent south of the Canadian Malartic deposit along a NW-SE trend from the Cartier zone to the Bravo zone. A total of 458 structural measurements shows that S_2 is broadly sub-vertical trending NW-SE, and that its orientation does not change significantly across the three structural domains. However, its orientation becomes NNW-SSE along a 2–3 km wide structural corridor west of the Canadian Malartic deposit (Fig. 6-B). A faint but systematic crenulation of S_2 is observed in this corridor and it appears to grossly bend S_2 in a clockwise fashion. At the outcrop scale, refraction of the S_2 foliation between the meta-sedimentary rock layers, the mafic and the felsic-intermediate dykes is common. S_2 is marked by biotite and white mica in the meta-sedimentary rocks and by biotite and amphibole in the meta-basic dykes.

L_2 stretching lineations are subtle and rarely seen because of the absence of clear preserved strain markers. Mineral lineations are generally marked by clusters of biotite but are difficult to differentiate from the intersection lineation between the S_2 and the crenulation cleavage. However, pseudomorphs of an early to *syn*-deformation metamorphic porphyroblast (replaced by biotite, white mica, ±quartz, ±calcite in the mineralized zones, Fig. 5-C) locally mark an obvious stretching lineation, which is parallel to the clusters of biotite. The average of 221 structural measurements indicates an overall E-W direction and a plunge of 64° to the east for the L_2 lineation (Fig. 6-C).

The S_3 crenulation cleavage is non penetrative, sub-vertical and mainly oriented NE-SW (Fig. 6-D). Several conjugate kink bands are marked by a crenulation of S_2, by quartz veinlets (locally strongly weathered) and by the replacement of staurolite porphyroblasts by an assemblage of chlorite, micas, ±epidote and ±quartz. The dominant orientation of the kinks is sub-parallel to the S_3 cleavage (Fig. 6-D).

3.3.5. Variations in the intensity of S_2

The field mapping in this study highlights partitioning of the intensity of the S_2 biotite foliation throughout the area (Fig. 8-A). The intensity of the S_2 foliation in greywackes was visually characterized as high where a strong pressure-solution cleavage and alignments of biotite mark the axial surface of F_2 folds (Fig. 8-B), as moderate where the pressure-solution cleavage is only visible within some high strain bands, and as low where only subtle alignments of biotite are visible (Fig. 8-C). Outcrops where S_2 is parallel to bedding (i.e., F_2 fold limbs) and those where bedding is invisible were not assessed in these terms.

Fig. 8-A represents observation points and a minimum-curvature interpolation of the apparent intensity of the S_2 foliation in greywackes (siltstone, mudstone and other lithologies are not considered here). Highest intensity zones are located in the vicinity of the Canadian Malartic deposit, in the north-west of the Cartier zone and in the west of the mapped area. Lower intensity zones are located in the east, south and west of Bob's dyke. Parameters that may have contributed to the variation of the apparent intensity of the S_2 foliation include the proximity of igneous rocks (meta-basic or felsic dykes), the earlier structures (e.g., F_1 fold hinges), the metamorphism, the changes in mineralogy due to pre-existing hydrothermal alteration and the Cadillac Larder Lake Deformation Zone. Igneous rocks and earlier structures may locally contribute to variations of the S_2 intensity in greywackes but not to the regional pattern. The overall distribution of the S_2 foliation intensity does not show a clear north-south variation and is therefore unlikely to be linked with increasing grade of metamorphism toward the south. Instead, high intensity zones around Canadian Malartic and along the Cadillac Larder Lake Deformation Zone in the north-west of the map (Fig. 8-A) could be linked to increasing strain with decreasing distance from the Cadillac Larder Lake Deformation Zone or to the presence of mineralizing fluids and/or zones of hydrothermal alteration in the vicinity of the Canadian Malartic deposit during D_2 (De Souza et al., 2016).

3.3.6. Metamorphism

The textural relationships between the metamorphic porphyroblasts and the S_2 foliation provide some constraints on the relative timing of the peak of metamorphism with respect to deformation. In the Central and South domains, staurolite poikiloblasts contain inclusion trails of biotite, white mica and quartz in continuity with the S_2 biotite foliation (Fig. 5-D) and therefore post-date the bulk of the D_2 deformation event. However, subtle rotations of the poikiloblasts have been observed at a few locations suggesting that the peak metamorphic conditions were syn- to late- D_2.

3.3.7. Veins

Gold-bearing and barren veins are abundant throughout the Canadian Malartic area and may provide critical information on the timing of intrusive rocks and ore forming processes. De Souza et al. (2015, 2016) reported 5 major vein generations in the Canadian Malartic deposit: three of them are interpreted to be *syn*-D_2 and associated with the main gold mineralization event hosted by both the meta-sedimentary and the intrusive rocks. Their two late vein sets are barren and cross-cut the S_2 foliation. In the Cartier area (Fig. 4), an early barren vein set is cross-cut by the quartz-monzodiorite intrusions and is interpreted to be pre- to early-D_2 (Blacklock, 2015). These are quartz ± feldspar tension-veins, millimeter to less than a meter thick that are perpendicular to the L_2 stretching lineation. They are slightly

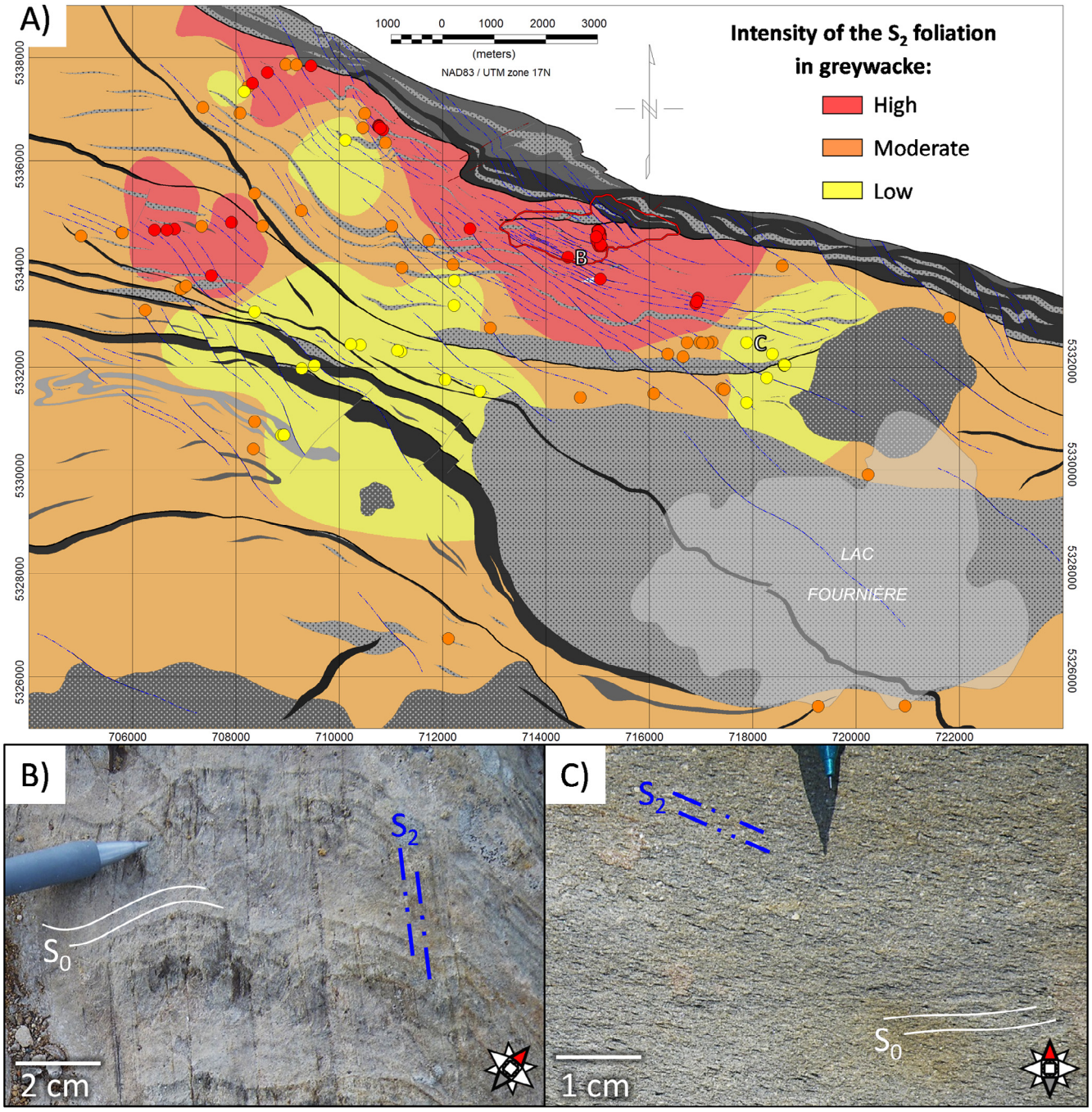

Fig. 8. Intensity of the S_2 foliation in greywackes. A) Interpolation of field observations (the grid and the colored points represent the same information). The coordinate system is NAD83-UTM17N. The red line represents the open-pit mine (as designed in 2013). Highest intensity of S_2 is in the vicinity of the Canadian Malartic deposit and in the west. Overall the intensity of the S_2 foliation decrease toward the south. B) High intensity end-member showing a strong pressure-solution cleavage and alignments of biotite. C) Low intensity end-member with subtle alignment of biotite. The few biotite grains that are sub-parallel to the bedding (S_0) in this photograph may correspond to remnant of the S_0-S_1 fabric.

deformed by F_2 folds and are cross-cut by meta-basic dykes and by a subtle S_2 foliation (Fig. 5-E). Their emplacement can therefore be interpreted to have occurred in dilation zones related to the onset of D_2, with an opening direction parallel to the L_2 stretching lineation. De Souza et al. (2016) described a similar vein set (i.e., their V_4 veins) in the Canadian Malartic deposit but interpreted it to be late D_2 in the absence of clear cross-cutting observations. Along the north wall of the Canadian Malartic open pit these veins and the Sladen intrusions display a similar west-dipping apparent geometry (Fig. 9-A). Observed cross-cutting relationship between the quartz-monzodiorite, these tension-veins, the meta-basic dykes and the S_2 foliation in the Canadian Malartic district reasonably suggest that the Sladen intrusions were emplaced prior to or in the early stage of the D_2 deformation event.

4. Evolution of the Canadian Malartic district

Based on the revised geological mapping and structural data compilation, three structural domains, three phases of

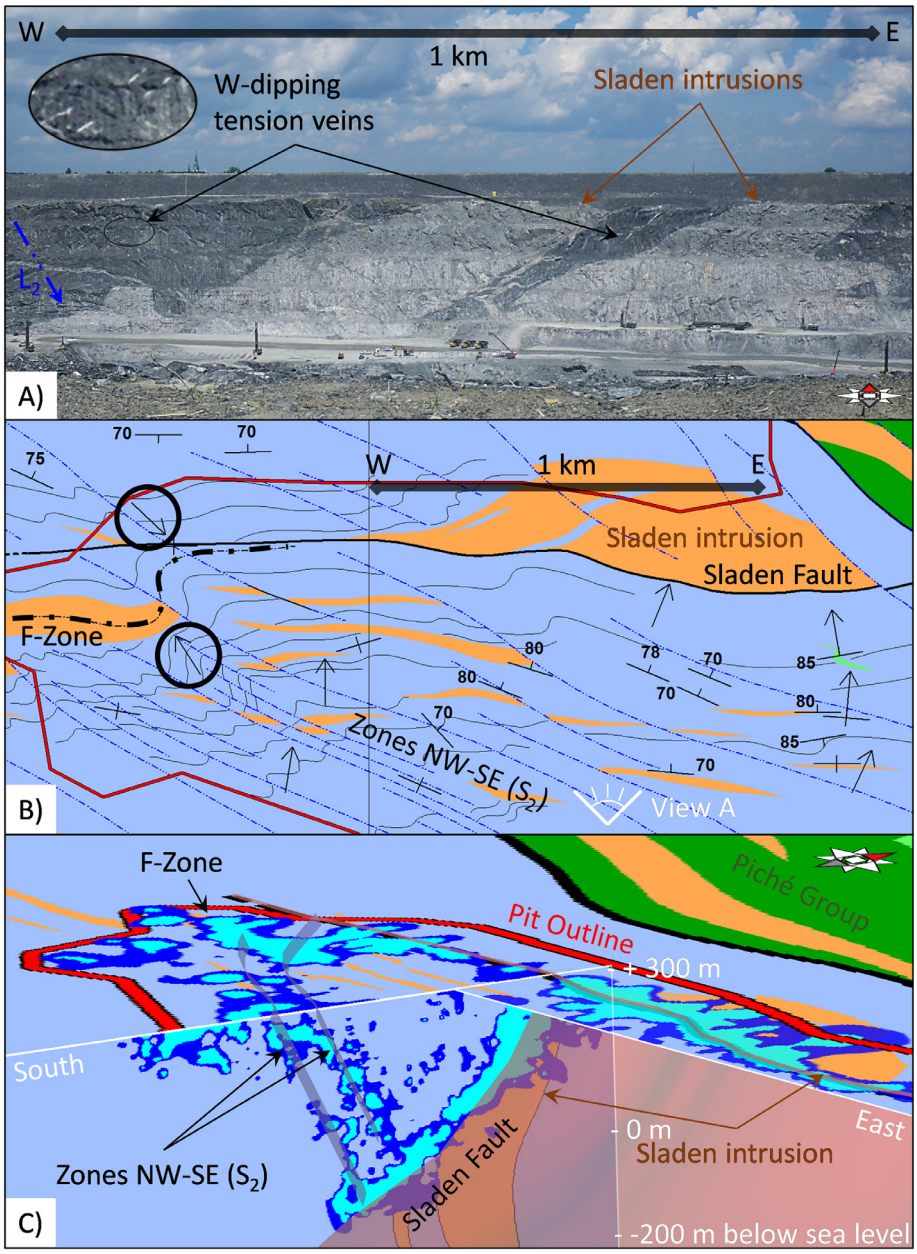

Fig. 9. A) Field photograph illustrating the west-dipping setting of some of the Sladen intrusions and of tension veins, that are perpendicular to the L_2 stretching lineation. B) Compiled structural map of the Canadian Malartic deposit. Location and legend are shown on Fig. 4. Traces of bedding are from Derry (1939) and Minerais Lac Limited (unpublished reports and maps). Younging direction are opposing on both side of the F-Zone intrusion, which suggests the presence of a major F_1 synform fold hinge. C) 3D view of gold assays in the Canadian Malartic deposit (dark blue >100 ppb, light blue >500 ppb). Mineralized rocks are mostly located at the contact with quartz-monzodiorite intrusion (e.g., F-Zone, Sladen Fault Zone). The absence of major intrusive rock contact results in a patchier gold distribution (e.g., in the NW-SE zones).

deformations, four phases of Archean magmatism, and one metamorphic episode are interpreted in the Pontiac Subprovince, south of Malartic. The North, Central and South domains underwent all the deformation events and were intruded by similar magmatic phases but, overall, the structural expression differs significantly between these domains. The North domain, which hosts the Canadian Malartic deposit, is structurally complex with numerous F_1 and F_2 fold interferences, resulting in significant variations of the bedding and younging orientations. By contrast, bedding in the Central domain is very homogeneous, with a sub-vertical orientation. The South domain has an intermediate structural complexity and hosts meta-volcanic rocks interlayered within meta-sedimentary rocks and iron formations. Metamorphic porphyroblasts (e.g., garnet and staurolite) are only observed in the Central and South domains. Camiré and Burg (1993) similarly interpreted two domains in the Pontiac Subprovince south of Rouyn-Noranda, referring to them as upper nappe (North domain herein) and a lower nappe (Central and South domains herein).

Four phases of magmatism occur in the area. Each phase relates to specific tectonic and metallogenic events in the Canadian Malartic district. Phase 1 magmatism (ca. 2683–2680 Ma, e.g., Lac Fournière plutons U-Pb zircon age determination at 2682.4 ± 1.0 Ma, Davis, 2002) immediately post-date the final stages of the sedimentation of the Pontiac Group (youngest detrital zircon U-Pb age at 2682.7 ± 1.9 Ma, Mortensen and Card, 1993. The Lac Fournière intrusions record the S_1 foliation (as marked by magnetic lineaments) and therefore formed before or during the onset of D_1, which may have facilitated and focused strain at the contact of

meta-sedimentary beds with plutonic masses that acted as rigid bodies. Isoclinal F_1 folding together with Phase 1 plutons conditioned the heterogeneous structural architecture of the northern part of the Pontiac Subprovince. D_1 also developed as the dominant foliation within the Cadillac Larder Lake Deformation Zone according to Bedeaux et al. (2017).

Phase 2 magmatism (ca. 2679–2676 Ma, Helt et al., 2014; De Souza et al., 2015, 2016) formed the major intrusive bodies that are spatially associated with gold at the Canadian Malartic deposit. The relative timing of these intrusions is mainly constrained by observations in the Cartier area, where they cross-cut pre- or early- D_2 veins, are cross-cut by the S2 foliation and are folded by F_2 (Blacklock, 2015). Geochronological data and cross-cutting field observations suggest that Phase 2 bodies were emplaced after D1 and early D_2 into the Pontiac meta-sedimentary rocks.

Phase 3 magmatism (ca. 2675–2673 Ma) produced basic dykes that intruded the Pontiac meta-sedimentary rocks. They may be contemporaneous with the deposition of Timiskaming-type sediments (<2676 Ma, U-Pb on detrital zircon, Pilote, 2014) in the north of the Cadillac Larder Lake Deformation Zone, where the basic dykes have not been observed. These dykes cross-cut the Phase 2 Sladen intrusions, are affected by F_2-folds and display the S_2 foliation, which is defined by metamorphic hornblende in the least altered dyke samples and by biotite in the hydrothermally altered dyke samples. These observations indicate that Phase 3 mafic dykes were emplaced, deformed, mineralized and metamorphosed during protracted stages of the D_2 deformation event.

Phase 4 magmatism is represented by the Décelles Batholith (ca. 2672–2662 Ma, based on monazite ages of Mortensen and Card, 1993). S-type granites and pegmatites are the dominant rock types in the southern part of the Pontiac Subprovince (Fig. 1) and are also present as dykes within the Pontiac meta-sedimentary rocks. Refraction of the S_2 biotite foliation in the vicinity of these dykes and open F_2 folds (Fig. 5-F) indicates that the Décelles magmatism also occurred before the end of D_2. Phase 4 magmatism is consequently older than, or coeval with, a syn- to late-D2 peak of metamorphism in the Pontiac Subprovince, and could be sourced from partial melting of the Pontiac meta-sedimentary rocks at depth during D_2 (Feng and Kerrich, 1991, 1992). Several felsic dykes in the North domain of the Pontiac Subprovince, in the vicinity of the Canadian Malartic deposit, could potentially be related with the Décelles magmatism. Furthermore, some magma-derived mineralizing fluids in the Canadian Malartic deposit (Helt et al., 2014) may also be linked to this magmatic event. The estimated age range for the Décelles Batholith is consistent with the possible age of mineralization at 2664 ± 11 Ma (re-Os on molybdenite, De Souza et al., 2015, 2016). A genetic link between auriferous fluids and the S-type magmatism was previously proposed in the southern Abitibi Subprovince (Olivo et al., 2007), however further investigation of the felsic dykes and of the Décelles Batholith is required to demonstrate their relationship.

The D_3 deformation event postdates the Décelles magmatism. Absolute timing of the subtle S_3 crenulation cleavage and of associated D_3 kinks has not yet been determined. This late deformation event is extensively documented in the Abitibi Subprovince and along the Cadillac Larder Lake Deformation Zone, where it shows Z-shaped folds and is interpreted as a dextral transcurrent phase (Daigneault et al., 2002; Lafrance, 2015; Bedeaux et al., 2017). Replacement of staurolite by chlorite, micas, epidote, ±quartz and biotite into chlorite along D_3 kinks and quartz veinlets indicates that the D_3 event postdates the peak of metamorphism and could represent regional cooling. Alternatively, it may correspond to a much younger event, Proterozoic ages being reported for parts of the southern Abitibi Subprovince (e.g., Zhang et al., 2014).

5. Structural controls of intrusive rocks and gold mineralization

A detailed structural map of the Canadian Malartic deposit (Fig. 9-B) has been interpreted from the compilation of historical dataset of Derry (1939) and Minerais Lac Limited (unpublished maps). Key features include the E-W Sladen Fault Zone, E-W quartz-monzodiorite bodies that are cross-cut and offset by NW-SE S_2-parallel high strain zones and fractures, a major S-shaped F_2 fold in the F-Zone and Gilbert Zone (De Souza et al., 2016), and numerous parasitic F_2 folds. Gold mineralization is interpreted to be primarily associated with the Sladen Fault Zone and with the NW-SE fractures (Derry, 1939; De Souza et al., 2015, 2016). Fig. 9-C illustrates these two major structural controls on the gold distribution in the Canadian Malartic deposit. The presence of intrusive rocks also provides a significant control on the mineralization, interpreted to be due to their competency and chemical contrasts with the host meta-sedimentary rocks.

In order to further evaluate the significance of the presence of intrusive rocks on gold mineralization in the Canadian Malartic district, we calculated the 3D Euclidian distance between each of the 526,000 gold assay and the nearest monzodiorite body. Fig. 10-A represents the distribution of the 364,000 gold assays above 10 ppb. 99% of them are within a 100 m radius from the nearest monzodiorite body, at an average distance of 19.2 m. The relative proportion of mineralized samples is maximal at the contact and within the intrusions, with around 16.5% of the analyses above 1000 ppb and 63.4% of the analyses above 100 ppb. These proportions respectively drop to 9.6% and 29.8% at 10 m from the contact (Fig. 10-A). These results quantitatively confirm the spatial association between gold mineralization and intrusive rocks in the Canadian Malartic district. Therefore, determining the spatial distribution of Phase 2 Sladen intrusions could be a prospectivity tool for Canadian Malartic style of mineralization in the Pontiac Subprovince.

The largest Phase 2 quartz-monzodiorite bodies are located in the footwall of the Sladen Fault Zone and to the west of the Canadian Malartic deposit (F-Zone, Fig. 9-B). Opposing younging directions of the bedding in F_2 fold hinges in meta-sedimentary rocks are observed between the two sides of the F-Zone intrusion, indicating that the intrusion is located in the hinge of a major F_1 fold. Similar spatial relationships between F_1 fold hinges and intrusive rocks were reported in the Canadian Malartic, Gouldie and Cartier zones (Sansfaçon and Hubert, 1990; Blacklock, 2015).

The variance of the bedding dip (Fig. 7) is an indicator of the structural complexity, with high variance calculated in the vicinity of fold hinges. Fig. 10-B and -C illustrate the relationships between the calculated variance of the bedding dip, the 3D Euclidian distance from the nearest gold value above 100 ppb, and the 3D Euclidian distance from the nearest quartz monzodiorite. The highest variance values are consistently distributed within a short distance from a monzodiorite body and from a gold mineralized area. These graphs (Fig. 10) support the visual interpretation of Fig. 7, which links high variance anomalies together with gold occurrences.

We propose that the geometry of the F_1 fold hinges spatially controlled the emplacement of Phase 2 intrusive bodies, while D_2 structures propagated in the North domain of the Pontiac Subprovince. During protracted D_2 tectonism, the high-strain Sladen Fault Zone was developed or reactivated along the southern contacts of the intrusions and propagated eastwards to "connect" with the proximal *trans*-crustal Cadillac Larder Lake Deformation Zone, which would have further contributed to channel mineralizing fluid flows along permeable brecciated zones as previously proposed by Derry (1939).

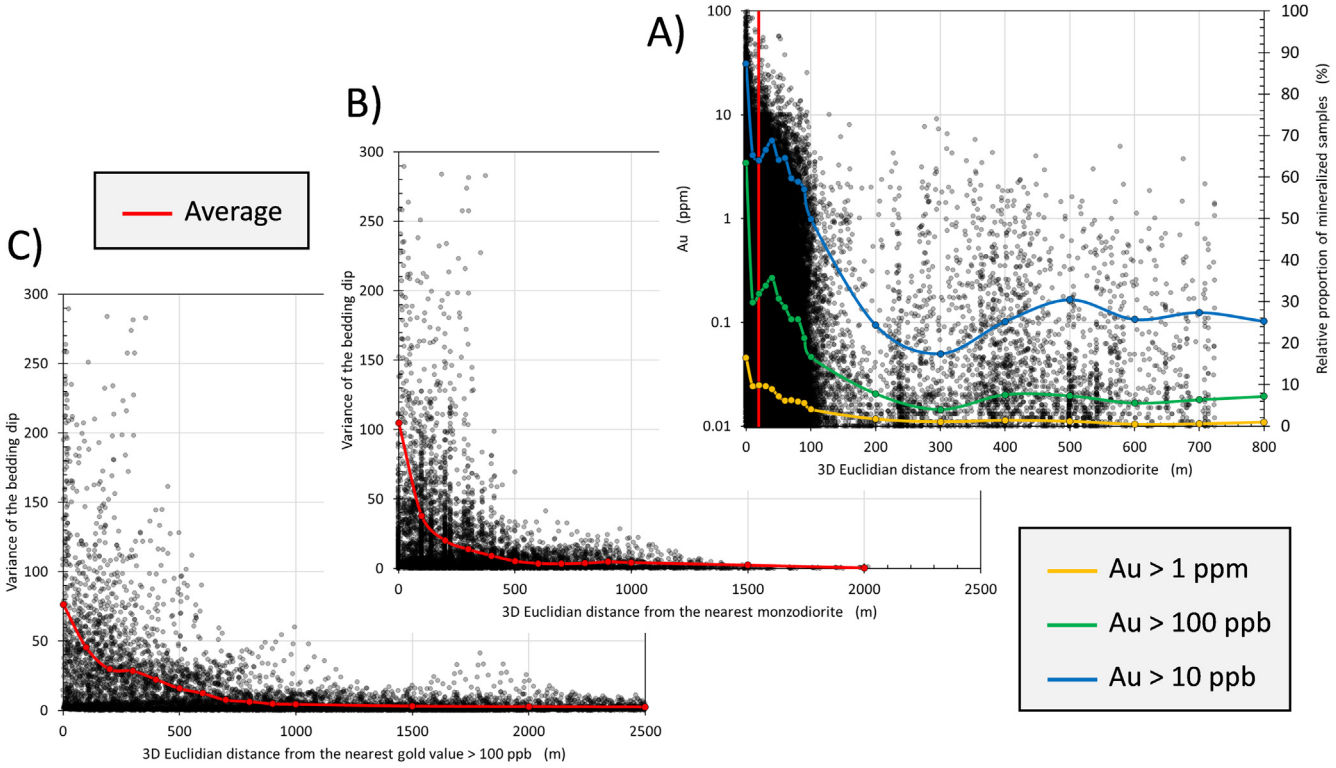

Fig. 10. A) Au content versus 3D Euclidian distance from the nearest monzodiorite intrusion. The red line represents the average distance of gold values above 10 ppb. The blue, green and yellow lines represent the proportion of mineralized meta-sedimentary rock samples which is maximal at the contact with a felsic-intermediate intrusive rock. B) C) Variance of the bedding dip (see Fig. 6 and text) versus 3D Euclidian distance from the nearest monzodiorite intrusion and from the nearest mineralized sample. High variance values are only observed within short distance from felsic-intermediate intrusive rocks and mineralized zones. (For interpretation of the references to color in this figure legend, the reader is referred to the web version of this article.)

meta-sedimentary rocks in the vicinity of Canadian Malartic deposit better recorded the D_2 deformation event (De Souza et al., 2015, 2016) than the rest of the Pontiac and Abitibi Subprovinces, where D_2 is expressed by rare S-shaped folds and a weak NW-SE steeply dipping S_2 foliation (D_3 of Bedeaux et al., 2017). Mapping indicates that penetrative S_2 foliation are restricted to the vicinity of the Canadian Malartic deposit (Fig. 8). Rheological differences of hydrothermally altered rocks in the footprint of the Canadian Malartic deposit, along with the presence of mineralizing fluids during D_2 (De Souza et al., 2016), likely strain softened the rock mass and facilitated re-orientation and crystallization of biotite along the S_2 fabric. The intensity of S_2 is therefore interpreted as evidence of *syn*-D_2 metasomatism.

The spatial distribution of F_1 fold hinges is considered a highly favorable "ground preparation" condition to focus dilation during D_2, to control the emplacement of Phase 2 quartz-monzodiorite intrusions, and to enhance further auriferous fluid circulation. Considering such relationship, the map of the variance of the bedding dip (Fig. 7) can be interpreted as a prospectivity map for Phase 2 Sladen intrusions, which develop rheology contrasts leading to gold mineralization. The magnitude of these favorable conditions are, altogether, enhanced close to the Cadillac Larder Lake Deformation Zone to develop mineralization of economic interest in the Pontiac Subprovince.

6. Conclusion

Airborne geophysical survey, field geological and structural observations, and previously published geochronological data were integrated to revise the geological map and to summarize the structural and magmatic history (Fig. 11) of the Pontiac Subprovince, south of the world-class Canadian Malartic gold deposit. Three structural domains, three phases of deformations, four phases of Archean magmatism, and one metamorphic event have been identified and allow the controls of gold mineralization in the Pontiac Subprovince to be better constrained.

Gold mineralization at Canadian Malartic is spatially associated with Phase 2 quartz-monzodioritic bodies that were emplaced within dilation zones in F_1 fold hinges during protracting D_2 deformation. The rheological contrast between the meta-sedimentary rocks and the Phase 2 quartz monzodiorite intrusions favored the propagation of the Sladen Fault Zone and its connectivity with the regional Cadillac Larder Lake Deformation Zone, which contributed to multi-stage fluid flow and enhanced the Canadian Malartic deposit gold endowment. Innovative quantitative structural approaches (i.e., calculation of the variance of the bedding dip and intensity of the S_2 foliation) combined with the identification of the spatial correlation between Phase 2 intrusions and the structural framework of the Pontiac Subprovince has led to a better understanding of the spatial distribution of these intrusions and of the role of their rheological contrasts with the meta-sedimentary host rocks, which controlled metasomatism and gold mineralization during D_2.

The visual estimation of the intensity of a foliation in a given lithology, although qualitative, may be a marker of local strain variations due to the proximity of a major crustal break (i.e. the Cadillac Larder Lake Deformation Zone), or of rheological preparation due to strain softening metasomatism (i.e. the Canadian Malartic footprint). Assuming statistically representative structural datasets, calculating the variance of the bedding could be a prospectivity criteria to explore for structurally complex zone, which potentially host mineralization in poly-deformed terranes.

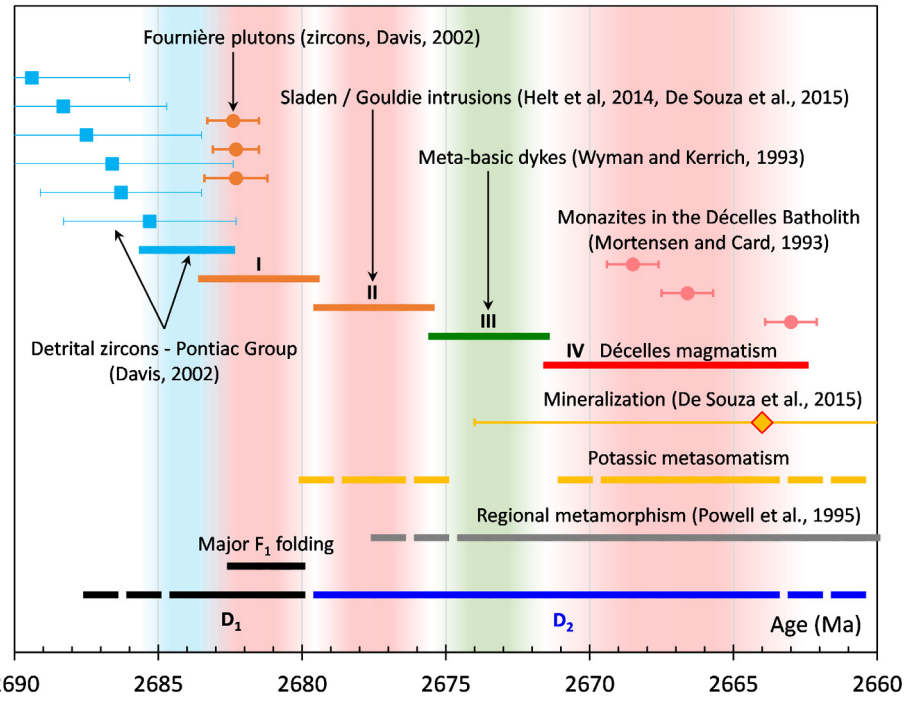

Fig. 11. Synthesis of the tectonic and magmatic evolution of the Pontiac Subprovince, south of Malartic. Four phases of mainly felsic-intermediate (in pink) or mainly mafic (in green, i.e., meta-basic dykes) magmatism can be distinguished. Mineralization, metasomatism, metamorphism and the D_2 deformation event are coeval. (For interpretation of the references to color in this figure legend, the reader is referred to the web version of this article.)

Acknowledgements

We are very grateful to Canadian Malartic Corporation, exploration and production departments, for their logistic support during field work, and particularly to Matthieu Dessureault, Alain Hébert, René De Carufel, Kayla Helt, François Bouchard, Christian Tessier, Marie-Claude Brunet-Ladrie and Donald Gervais. We also would like to thank TGI-4 researchers, Stéphane De Souza, Benoit Dubé, Patrick Mercier-Langevin and Randolph J. Enkin, and MERNQ geologists, Pierre Pilote and Patrice Roy, for valuable discussions. Thanks to Bruno Lafrance and Robin Armit for the constructive reviews. Thanks to Robert Wares who helped initiating this research project. Finally, thanks to the Mineral Exploration Footprints Research Network (http://www.cmic-footprints.ca/). Funding was provided by the Natural Sciences and Engineering Council of Canada and the Canada Mining Innovation Council through the NSERC Collaborative Research and Development Program. NSERC-CMIC Mineral Exploration Footprints Project Contribution 104.

References

Banas and Melchiorre, 1998. Ressources Dianor Inc. Report, Ministère des Ressources Naturelles du Québec, GM 56443, p. 38.
Beaudoin, G., Raskevicius, T., 2014. Constraints on the genesis of the Archean oxidized, intrusion-related canadian malartic gold deposit, Quebec, Canada – a discussion. Econ. Geol. 109, 2067–2071.
Bedeaux, P., 2012. Minéralisations et deformation à proximité de la faille de Davidson, Abitibi, Canada (MSc thesis). Université du Québec à Chicoutimi. 239 p.
Bedeaux, P., Pilote, P., Daigneault, R., Rafini, S., 2017. Synthesis of the structural evolution and associated gold mineralization of the Cadillac Fault, Abitibi, Canada. Ore Geol. Rev. 82, 49–69.
Benn, K., Miles, W., Ghassemi, M.R., Gillet, J., 1993. Crustal structure and kinematic framework of the northwestern Pontiac Subprovince, Quebec: an integrated structural and geophysical study. Can. J. Earth Sci. 31, 271–281.
Bérubé, 1962. East Sullivan Mines Limited Report. Ministère des Ressources Naturelles du Québec. GM 12720, p.10.
Betts, P., Valenta, R.K., Finlay, J., 2003. Evolution of the Mount Woods Inlier, northern Gawler Craton, Southern Australia: an integrated structural and aeromagnetic analysis. Tectonophysics 366, 83–111.
Betts, P., Williams, H., Stewart, J., Aillères, L., 2007. Kinematic analysis of aeromagnetic data: looking at geophysical data in a structural context. Gondwana Res. 11, 582–583.
Blacklock, N., 2015. Vein Characterization Using Structural Controls and Petrographic Analysis at Cartier Zone in the Canadian Malartic Property at Malartic (BSc. Thesis). Queen's University, p. 68.
Briggs, I.C., 1974. Machine contouring using minimum curvature. Geophysics 39 (1), 39–48.
Buchan, K.L., Ernst, R.E., 2004. Diabase dyke swarms and related units in Canada and adjacent regions. Geological Survey of Canada. Map 2022A, scale 1:5000000.
Buchan, K.L., Mortensen, J.K., Card, K.D., 1993. Northeast-trending Early Proterozoic dykes of southern Superior Province: multiple episodes of emplacement recognized from integrated paleomagnetism and U-Pb geochronology. Can. J. Earth Sci. 30, 1286–1296.
Camiré, G.E., Burg, J.P., 1993. Late Archean thrusting in the northwestern Pontiac Subprovince, Canadian Shield. Precambrian Res. 61, 51–66.
Camiré, G.E., Laflèche, M.R., Ludden, J.N., 1993a. Archean metasedimentary rocks from the northwestern Pontiac Subprovince of the Canadian Shield: chemical characterization, weathering and modelling of the source areas. Precambrian Res. 62, 285–305.
Camiré, G.E., Ludden, J.N., La Fleche, M.R., Burg, J.P., 1993b. Mafic and ultramafic amphibolites from the northwestern Pontiac Subprovince: chemical characterization and implications for tectonic setting. Can. J. Earth Sci. 30, 1110–1122.
Card, K.D., 1990. A review of the Superior Province of the Canadian Shield, a product of Archean accretion. Precambrian Res. 48, 99–156.
Chown, E.H., Harrap, R., Moukhsil, A., 2002. The role of granitic intrusions in the evolution of the Abitibi belt, Canada. Precambrian Res. 115, 291–310.
Corfu, F., Noble, S.R., 1992. Genesis of the southern Abitibi greenstone belt, Superior Province, Canada: evidence from zircon Hf isotope analyses using a single filament technique. Geochim. Cosmochim. Acta 56, 2081–2097.
Daigneault, R., Mueller, W.U., Chown, E.H., 2002. Oblique Archean subduction: accretion and exhumation of an oceanic arc during dextral transpression, Southern Volcanic Zone, Abitibi Subprovince Canada. Precambrian Res. 115, 261–290.
D'Amours, I., Intissar, R., 2012. Levé magnétique héliporté dans le secteur de Malartic, Abitibi. Ministère des Ressources Naturelles du Québec. DP 2012-04.
Davis, D., 2002. U-Pb geochronology of Archean metasedimentary rocks in the Pontiac and Abitibi subprovinces, Québec, constraints on timing, provenance and regional tectonics. Precambrian Res. 115, 97–117.
De Souza, S., Dubé, B., McNicoll, V.J., Dupuis, C., Mercier-Langevin, P., Creaser, R.A., Kjarsgaard, I.M., 2015. Geology, hydrothermal alteration, and genesis of the world-class Canadian Malartic stockwork-disseminated Archean gold deposit, Abitibi, Quebec. In: Dubé, B., Mercier-Langevin, P. (Eds.), Targeted Geoscience

Initiative 4: Contributions to the Understanding of Precambrian Lode Gold Deposits and Implications for Exploration. Geological Survey of Canada, pp. 113–126. Open File 7852.
De Souza, S., Dubé, B., McNicoll, V.J., Dupuis, C., Mercier-Langevin, P., Creaser, R.A., Kjarsgaard, I.M., 2016. Geology and hydrothermal alteration of the world-class Canadian malartic gold deposit: genesis of an Archean stockwork-disseminated gold deposit in the Abitibi Greenstone Belt, Québec. Econ. Geol. Rev. 19, p. 29, in press.
Derry, D.R., 1939. The geology of the Canadian Malartic gold mine, N. Quebec. Econ. Geol. 34, 495–523.
Desrochers, J.P., Hubert, C., 1996. Structural evolution and early accretion of the Archean Malartic Composite Block, southern Abitibi greenstone belt, Quebec, Canada. Can. J. Earth Sci. 33, 1556–1569.
Dimroth, E., Imreh, L., Goulet, N., Rocheleau, M., 1983. Evolution of the south-central segment of the Archean Abitibi Belt, Québec. Part II: tectonic evolution and geomechanical model. Can. J. Earth Sci. 20, 1355–1373.
Dion, D.J., Lefebvre, D., 1997. Données numériques (profils) des levés geophysiques aéroportés du Québec – SNRC 32D. Ministère des Ressources Naturelles du Québec. DP 96-02.
Dubé, B., Gosselin, P., Mercier-Langevin, P., Hannington, M., Galley, A., 2007. Gold-rich volcanogenic massive sulphide deposits. In: Goodfellow, W.D. (Ed.), Mineral Deposits of Canada: A Synthesis of Major Deposit-Types, District Metallogeny, the Evolution of Geological Provinces, and Exploration Methods. Geological Association of Canada, Mineral Deposits Division, pp. 75–94. Special Publication 5.
Dubé, B., Gosselin, P., 2007. Greenstone-hosted quartz-carbonate vein deposits. In: Goodfellow, W.D. (Ed.), Mineral Deposits of Canada: A Synthesis of Major Deposit Types, District Metallogeny, the Evolution of Geological Provinces, and Exploration Methods. Geological Association of Canada, Mineral Deposits Division, pp. 49–73. Special Publication 5.
Enkin, R.J., Cowan, D., Tigner, J., Severide, A., Gilmour, D., Tkachyk, A., Kilduff, M., Vidal, B., Baker, J., 2012. Physical Property Measurements at the GSC Paleomagnetism and Petrophysics Laboratory, including Electric Impedance Spectrum Methodology and Analysis. Geological Survey of Canada. Open File 7227, p. 42.
Ernst, R.E., 1994. Mapping the magma flow pattern in the Sudbury dyke swarm in Ontario using magnetic fabric analysis. In: Current Research 1994-E. Geological Survey of Canada, pp. 183–192.
Ernst, R.E., Buchan, K.L., 1993. Paleomagnetism of the Abitibi dyke swarm, southern Superior Province, and implications for the Logan Loop. Can. J. Earth Sci. 30, 1886–1897.
Fallara, F., Ross, P.S., Sansfaçon, R., 2000. Caractérisation géochimique, pétrographique et structurale: nouveau modèle métallogénique du camp minier de Malartic. Ministère des Ressources Naturelles du Québec. MB 2000-15, p. 161.
Feng, R., Kerrich, R., 1991. Single zircon age constraints on the tectonic juxtaposition of the Archean Abitibi greenstone belt and Pontiac subprovince, Quebec, Canada. Geochim. Cosmochim. Acta 55, 3437–3441.
Feng, R., Kerrich, R., 1992. Geochemical evolution of granitoids from the Archean Abitibi Southern Volcanic Zone and the Pontiac subprovince, Superior Province, Canada: implications for tectonic history and source regions. Chem. Geol. 98, 23–70.
Feng, R., Kerrich, R., McBride, S., Farrar, E., 1992. 40Ar/39Ar age constraints on the thermal history of the Archean Abitibi greenstone belt and the Pontiac Subprovince: implications for terrane collision, differential uplift and overprinting of gold deposits. Can. J. Earth Sci. 29, 1389–1411.
Feng, R., Kerrich, R., Maas, R., 1993. Geochemical, oxygen, and neodymium isotope compositions of metasediments from the Abitibi greenstone belt and Pontiac Subprovince, Canada: evidence for ancient crust and Archean terrane juxtaposition. Geochim. Cosmochim. Acta 57, 641–658.
Gagnier, 1997. Explorations Malartic Sud Inc. Report, Ministère des Ressources Naturelles du Québec, GM 55484, p. 263.
Gariépy, C., Allègre, C.J., Lajoie, J., 1984. U-Pb systematics in single zircons from the Pontiac metasediments, Abitibi greenstone belt. Can. J. Earth Sci. 21, 1296–1304.
Gervais, D., Roy, C., Thibault, A., Pednault, C., Doucet, D., 2014. Technical Report on the Mineral Resource and Mineral Reserve Estimates for the Canadian Malartic Property. Mine Canadian Malartic. 460 p.
Gunning, H.C., Ambrose, J.W., 1940. Malartic area, Quebec. Geological Survey of Canada. Memoir 222, p. 151.
Helt, K.M., Williams-Jones, A.E., Clark, J.R., Wing, B.A., Wares, R.P., 2014. Constraints on the Genesis of the Archean Oxidized, Intrusion-Related Canadian Malartic Gold Deposit, Quebec, Canada. Econ. Geol. 109, 713–735.
Jolly, W.T., 1980. Development and degradation of Archean lavas, Abitibi Area, Canada, in light of major element geochemistry. J. Petrol. 21 (2), 323–363.
Lafrance, B., 2015. Geology of the orogenic Cheminis gold deposit along the Larder Lake – Cadillac deformation zone, Ontario. Can. J. Earth Sci. 52, 1093–1108.
MacLeod, I.N., Jones, K., Fan Dai, T., 1993. 3-D analytic signal in the interpretation of total magnetic field data at low magnetic latitudes. Explor. Geophys. 24, 679–688.
Mercier-Langevin, P., Dubé, B., Lafrance, B., Hannington, M., Galley, A., Moorhead, J., Gosselin, P., 2007. Metallogeny of the Doyon-Bousquet-LaRonde mining camp, Abitibi Greenstone Belt, Quebec. In: Goodfellow, W.D. (Ed.), Mineral Deposits of Canada: A Synthesis of Major Deposit-Types, District Metallogeny, the Evolution of Geological Provinces, and Exploration Methods. Geological Association of Canada, Mineral Deposits Division, pp. 673–701. Special Publication 5.
Morasse, S., Wasteneys, H.A., Cormier, M., Helmstaedt, H., Mason, R., 1995. A pre-2686 Ma intrusion-related gold deposit at the Kiena mine, Val d'Or, Québec, southern Abitibi Subprovince. Econ. Geol. 90, 1310–1321.
Mortensen, J.K., Card, K.D., 1993. U-Pb age constraints for the magmatic and tectonic evolution of the Pontiac Subprovince, Quebec. Can. J. Earth Sci. 30, 1970–1980.
Neumayr, P., Hagemann, S.G., Couture, J.F., 2000. Structural setting, textures, and timing of hydrothermal vein systems in the Val d'Or camp, Abitibi, Canada: implications for the evolution of transcrustal, second- and third-order fault zones and gold mineralization. Can. J. Earth Sci. 37, 95–114.
Olivo, G.R., Williams-Jones, A.E., 2002. Genesis of the Auriferous C Quartz-Tourmaline Vein of the Siscoe Mine, Val d'Or District, Abitibi Subprovince, Canada: Structural, Mineralogical and Fluid Inclusion Constraints. Econ. Geol. 97, 929–947.
Olivo, G.R., Chang, F., Kyser, T.K., 2006. Formation of the Auriferous and Barren North Dipper Veins in the Sigma Mine, Val d'Or, Canada: constraints from structural, mineralogical, fluid inclusion, and isotopic data. Econ. Geol. 101, 607–631.
Olivo, G.R., Isnard, H., Williams-Jones, A.E., Gariépy, C., 2007. Pb isotope compositions of pyrite from the C Quartz-Tourmaline Vein of the Siscoe Gold Deposit, Val d'Or, Quebec: constraints on the origin and age of the gold mineralization. Econ. Geol. 102, 137–146.
Perrouty, S., Aillères, L., Jessell, M.W., Baratoux, L., Bourassa, Y., Crawford, B., 2012. Revised Eburnean Geodynamic Evolution of the Gold-rich Southern Ashanti Belt, Ghana, with new Field and Geophysical Evidence of pre-Tarkwaian Deformations. Precambrian Res. 204–205, 12–39.
Perrouty, S., Lindsay, M.D., Jessell, M.W., Aillères, L., Martin, R., Bourassa, Y., 2014. 3D modeling of the Ashanti Belt, southwest Ghana: Evidence for a litho-stratigraphic control on gold occurrences within the Birimian Sefwi Group. Ore Geol. Rev. 63, 252–264.
Perrouty, S., Linnen, R.L., Lypaczewski, P., Gaillard, N., Olivo, G.R., Lesher, C.M., Piette-Lauzière, N., Crocker, M., Piercey, S.J., El Goumi, N., Enkin, R.J., Bouchard, F., 2015, Footprint of the Canadian Malartic Gold Deposit, QC, Canada: Preliminary Evaluation of Mafic Dyke Alteration. Extended Abstract. 13th SGA Biennial Meeting, 24–27 August 2015, Nancy, France, 3 p.
Pilote, P., 2014. Géologie Malartic. Ministère des Ressources Naturelles du Québec. MB 2000-09, Map CG-32D01D-2013-01, scale 1:20000.
Pilote, P., Beaudoin, G., Chabot, F., Crevier, M., Desrochers, J.P., Giovenazzo, D., Lavoie, S., Moorhead, J., Mueller, W., Pelz, P., Robert, F., Scott, C., Tremblay, A., Vorobiev, L., 2000. Géologie de la région de Val d'Or, Sous-province de l'Abitibi – Volcanologie physique et évolution métallogénique. Ministère des Ressources Naturelles du Québec. MB 2000-09, p. 116.
Powell, W.G., Carmichael, D.M., Hodgson, C.J., 1995. Conditions and timing of metamorphism in the southern Abitibi greenstone belt, Québec. Can. J. Earth Sci. 32, 787–805.
Rajagopalan, S., Milligan, P., 1994. Image enhancement of aeromagnetic data using automatic gain control. Explor. Geophys. 25, 173–178.
Rive, M., Pintson, H., Ludden, J.N., 1990. Characteristics of late Archaean plutonic rocks from the Abitibi and Pontiac subprovinces, Superior Province, Canada. In: Rive, M., Verpealst, P., Gagnon, Y., Lulin, J.M., Riverin, G., Simard, A. (Eds.), The northwestern Quebec polymetallic belt: A summary of 60 years of mining exploration, Special Vol. 43. The Canadian Institute of Mining and Metallurgy, pp. 65–76.
Robert, F., 2001. Syenite-associated disseminated gold deposits in the Abitibi greenstone belt, Canada. Miner. Deposita 36, 503–516.
Robert, F., Brown, A.C., 1986a. Archean gold-bearing quartz veins at the sigma mine, Abitibi Greenstone Belt, Quebec: Part I. Geologic relations and formation of the vein system. Econ. Geol. 81, 578–592.
Robert, F., Brown, A.C., 1986b. Archean gold-bearing quartz veins at the sigma mine, Abitibi Greenstone Belt, Quebec: Part II. Vein paragenesis and hydrothermal alteration. Econ. Geol. 81, 593–616.
Robert, F., Poulsen, K.H., 1997. World-class Archaean gold deposits in Canada: an overview. Aust. J. Earth Sci. 44, 329–351.
Sansfaçon, R., Grant, M., Trudel, P., 1987. Géologie de la mine Canadian Malartic, District de Val-d'Or. Ministère des Ressources Naturelles du Québec. MB 87-26, p. 49.
Sansfaçon, R., Hubert, C., 1990. The Malartic Gold District, Abitibi greenstone belt, Québec: Geological setting, structure and timing of gold emplacement Barnat, East- Malartic, Canadian Malartic and Sladen Mines. In: Rive, M., Verpealst, P., Gagnon, Y., Lulin, J.M., Riverin, G., Simard, A. (Eds.), The northwestern Quebec polymetallic belt: a summary of 60 years of mining exploration, Special Vol. 43. Canadian Institute of Mining and Metallurgy, pp. 221–235.
Stevenson, R.K., Patchett, P.J., 1990. Implications for the evolution of continental crust from Hf isotope systematics of Archean detrital zircons. Geochim. Cosmochim. Acta 54, 1683–1697.
Verduzco, B., Fairhead, J.D., Green, C.M., 2004. New insights into magnetic derivatives for structural mapping. Lead. Edge 29 (1), 24–29.
Wyman, D.A., Kerrich, R., 1993. Archean shoshonitic lamprophyres of the Abitibi Subprovince, Canada: petrogenesis, age, and tectonic setting. J. Petrol. 34 (6), 1067–1109.
Wyman, D.A., Kerrich, R., Polat, A., 2002. Assembly of Archean cratonic mantle lithosphere and crust: plume–arc interaction in the Abitibi-Wawa subduction–accretion complex. Precambrian Res. 115, 37–62.
Zhang, J., Linnen, R., Lin, S., Davis, D., Martin, R., 2014. Paleoproterozoic hydrothermal reactivation in a neoarchean orogenic lode-gold deposit of the southern Abitibi subprovince: U-Pb monazite geochronological evidence from the Young-Davidson mine, Ontario. Precambrian Res. 249, 263–272.